QC
851
.U65
no.46

PB92-137843

NOAA Technical Report, NWS 46

Functional Precision of National Weather Service Upper-Air Measurements Using Space Data Division Radiosonde (Model 909-10-01)

Silver Spring, Md.
October 1991

LIBRARY

N.O.A.A.
U.S. Dept. of Commerce

U.S. DEPARTMENT OF COMMERCE
National Oceanic and Atmospheric Administration
National Weather Service

REPRODUCED BY
U.S. DEPARTMENT OF COMMERCE
NATIONAL TECHNICAL
INFORMATION SERVICE
SPRINGFIELD, VA 22161

NOAA TECHNICAL REPORTS
National Weather Service Series

The National Weather Service (NWS) observes and measures atmospheric phenomena; develops and distributes forecasts of weather conditions and warnings of adverse weather; collects and disseminates weather information to meet the needs of the public and specialized users. The NWS develops the national meteorological service system and improves procedures, techniques, and dissemination for weather and hydrologic measurements, and forecasts.

NWS series of NOAA Technical Reports is a continuation of the former series, ESSA Technical Report Weather Bureau (WB).

Reports listed below are available from the National Technical Information Service, U.S. Department of Commerce, Sills Bldg., 5285 Port Royal Road, Springfield, VA 22161. Prices vary. Order by accession number (given in parentheses).

ESSA Technical Reports

WB 1 Monthly Mean 100-, 50-, 30-, and 10-Millibar Charts January 1964 through December 1965 of the IQSY Period. Staff, Upper Air Branch, National Meteorological Center, February 1967, 7 p, 96 charts. (AD 651 101)

WB 2 Weekly Synoptic Analyses, 5-, 2-, and 0.4-Mb Surfaces for 1964 (based on observations of the Meteorological Rocket Network during the IQSY). Staff, Upper Air Branch, National Meteorological Center, April 1967, 16 p, 160 charts. (AD 652 696)

WB 3 Weekly Synoptic Analyses, 5-, 2-, and 0.4-Mb Surfaces for 1965 (based on observations of the Meteorological Rocket Network during the IQSY). Staff, Upper Air Branch, National Meteorological Center, August 1967, 173 p. (AD 662 053)

WB 4 The March-May 1965 Floods in the Upper Mississippi, Missouri, and Red River of the North Basins. J. L. H. Paulhus and E. R. Nelson, Office of Hydrology, August 1967, 100 p.

WB 5 Climatological Probabilities of Precipitation for the Conterminous United States. Donald L. Jorgenson, Techniques Development Laboratory, December 1967, 60 p.

WB 6 Climatology of Atlantic Tropical Storms and Hurricanes. M. A. Alaka, Techniques Development Laboratory, May 1968, 18 p.

WB 7 Frequency and Areal Distributions of Tropical Storm Rainfall in the United States Coastal Region on the Gulf of Mexico. Hugo V. Goodyear, Office of Hydrology, July 19968, 33 p.

WB 8 Critical Fire Weather Patterns in the Conterminous United States. Mark J. Schroeder, Weather Bureau, January 1969, 31 p.

WB 9 Weekly Synoptic Analyses, 5-, 2-, and 0.4-Mb Surfaces for 1966 (based on meteorological rocket-sonde and high-level rawinsonde observations). Staff, Upper Air Branch, National Meteorological Center, January 1969, 169 p.

WB 10 Hemispheric Teleconnections of Mean Circulation Anomalies at 700 Millibars. James F. O'Connor, National Meteorological Center, February 1969, 103 p.

WB 11 Monthly Mean 100-, 50-, 30-, and 10-Millibar Charts and Standard Deviation Maps, 1966-1967. Staff, Upper Air Branch, National Meteorological Center, April 1969, 124 p.

WB 12 Weekly Synoptic Analyses, 5-, 2-, and 0.4-Millibar Surfaces for 1967. Staff, Upper Air Branch, National Meteorological Center, January 1970, 169 p.

NOAA Technical Reports

NWS 13 The March-April 1969 Snowmelt Floods in the Red River of the North, Upper Mississippi, and Missouri Basins. Joseph L. H. Paulhus, Office of Hydrology, October 1970, 92 p.

NWS 14 Weekly Synoptic Analyses, 5-, 2-, and 0.4-Millibar Surfaces for 1968. Staff, Upper Air Branch, National Meteorological Center, May 1971, 169 p. (COM-71-50383)

NWS 15 Some Climatological Characteristics of Hurricanes and Tropical Storms, Gulf and East Coasts of the United States. Francis P. Ho, Richard W. Schwerdt, and Hugo V. Goodyear, May 1975, 87 p. (COM-75-11088)

NWS 16 Storm Tide Frequencies on the South Carolina Coast. Vance A. Myers, June 1975, 79 p. (COM-75-11335)

NWS 17 Estimation of Hurricane Storm Surge in Apalachicola Bay, Florida. James E. Overland, June 1975. 66 p. (COM-75-111332)

(Continued on last page)

BIBLIOGRAPHIC INFORMATION

PB92-137843

Report Nos: NOAA-TR-NWS-46

Title: Functional Precision of National Weather Service Upper-Air Measurements Using Space Data Division Radiosonde (Model 9Ø9-1Ø-Ø1).

Date: Oct 91

Authors: P. Ahnert, M. Gelman, and M. Lukes.

Performing Organization: National Weather Service, Silver Spring, MD.**National Meteorological Center, Washington, DC.

Type of Report and Period Covered: Technical rept.

Supplementary Notes: See also PB92-137868 and PB92-13785Ø. Prepared in cooperation with National Meteorological Center, Washington, DC.

NTIS Field/Group Codes: 55D, 55C

Price: PC AØ3/MF AØ1

Availability: Available from the National Technical Information Service, Springfield, VA. 22161

Number of Pages: 49p

Keywords: *Meteorological instruments, *Radiosondes, Balloon-borne instruments, Acceptance tests, Atmospheric temperature, Temperature measurement, Humidity measurement, Barometric pressure, Troposphere, Precision, Comparison.

Abstract: The functional precision of Space Data Corporation Model 9Ø9-1Ø-Ø1 (SDC) radiosonde was determined using the National Weather Service functional analysis test package. The comparisons were made from 45 flights of paired radiosondes suspended from the same balloon. The two sondes were vertically separated by about 1Ø meters and, for the report, functional precision is given by the standard deviation of the differences (sigma-D) between measurements made by 2 sensors of the same type exposed to the same environment. Results are summarized for simultaneous measurements at one minute intervals as well as measurements at a predefined set of pressure levels. These tests were conducted for the acceptance of contract production samples and results are reported here for use by the meteorological community in specifying the characteristics of this radiosonde which began operational use in February of 1989.

PB92-137843

NOAA Technical Report, NWS 46

Functional Precision of National Weather Service Upper-Air Measurements Using Space Data Division Radiosonde (Model 909-10-01)

Office of Systems Operations
Engineering Division
Test and Evaluation Branch
Sterling, Va.
October 1991

QC
851
.U65
no.46

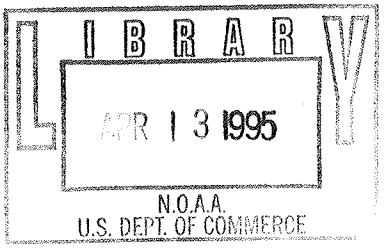

U.S. DEPARTMENT OF COMMERCE
Robert A. Mosbacher, Sr.; Secretary

National Oceanic and Atmospheric Administration
William E. Evans; Under Secretary

National Weather Service
Elbert W. Friday, Jr.; Assistant Administrator

ACKNOWLEDGEMENTS

Test report creation is credited to Peter Ahnert, currently at the NWS Weather Service Office in Harrisburg, PA. Extensive critical review and contributions are credited to Mel Gelman at the National Meteorological Center, Climate Analysis Center in Camp Springs, MD. Revision to final draft and publication arrangements are credited to Mike Lukes of NWS Test and Evaluation Branch at Sterling Research and Development Center, Sterling, VA.

Radiosonde flights and data processing were performed by the Test Branch of T&EB. Special thanks to Jim Fitzgibbon, Gene Hollingsworth, Dick Bollinger and Mike Ross for their long hours and dedication resulting in high quality data. Excellent maintenance support was provided by Dean Carson, of the T&EB Support Branch. Many others at T&EB also made contributions. The integrated functional test software, which made the detailed analysis of the data possible, was developed by Peter Hammett of the Network Software Branch, Office of System Operations (OSO). Thanks also to Joe Facundo of the Observing Systems Branch, OSO for his support and assistance.

TABLE OF CONTENTS

ACKNOWLEDGEMENTS iii

LIST OF FIGURES v

LIST OF TABLES v

ABSTRACT iv

1. BACKGROUND 1

2. INSTRUMENT DESCRIPTION 3

3. TEST METHODOLOGY 5
   3.1 RADIOSONDE PREPARATION/RELEASE 5
   3.2 GROUND EQUIPMENT 5
   3.3 DATA REDUCTION 6

4. COMPARISON BY TIME 8
   4.1 PRESSURE 8
   4.2 TEMPERATURE 10
   4.3 HUMIDITY 11
   4.5 HEIGHT 13

5. COMPARISON BY PRESSURE 25
   5.1 TEMPERATURE 25
   5.2 HUMIDITY 26
   5.3 HEIGHT 27

6. SUMMARY/CONCLUSIONS 37

7. REFERENCES 38

APPENDIX 39

LIST OF FIGURES

Figure 1 - Histogram of Pressure Differences by Time 14
Figure 2 - Scatter Plot of Pressure by Time 15
Figure 3 - Mean Differences of Pressure by Time 16
Figure 4 - Histogram of Temperature Differences by Time . . . 17
Figure 5 - Scatter Plot of Temperature by Time 18
Figure 6 - Mean Difference of Temperature by Time 19
Figure 7 - Histogram of Humidity Differences by Time 20
Figure 8 - Scatter Plot of Humidity by Time 21
Figure 9 - Mean Difference of Humidity by Time 22
Figure 10 - Histogram of T_d Differences by Time 23
Figure 11 - Scatter Plot of Height by Time 24
Figure 12 - Histogram of Temperature Difference by Pressure . 28
Figure 13 - Scatter Plot of Temperature by Pressure 29
Figure 14 - Histogram of Humidity Difference by Pressure . . . 30
Figure 15 - Scatter Plot of Humidity Difference by Pressure . 31
Figure 16 - Histogram of T_d Differences by Pressure 32
Figure 17 - Scatter Plot of Height by Pressure 33
Figure A1 - Illustration of SDC (Model 909-10-01) sonde . . . A1
Figure A2 - Pressure Difference v. Time for Flight 383 . . . . A2
Figure A3 - Temperature and Humidity v. Time for Flight 383 . A2
Figure A4 - Temperature and Humidity v. Time for Flight 291 . A3

LIST OF TABLES

Table 1 - Interval Statistics of Pressure by Time 13
Table 2 - Overall Statistics of Pressure by Time 14
Table 3 - WMO Interval Statistics of Pressure by Time 15
Table 4 - Interval Statistics of Temperature by Time 16
Table 5 - Overall Statistics of Temperature by Time 17
Table 6 - WMO Interval Statistics of Temperature by Time . . . 18
Table 7 - Interval Statistics of Humidity by Time 19
Table 8 - Overall Statistics of Humidity by Time 20
Table 9 - WMO Interval Statistics of Humidity by Time 21
Table 10 - Interval Statistics of T_d Depression by Time . . . 22
Table 11 - Overall Statistics of Height by Time 23
Table 12 - Interval Statistics of Temperature by Pressure . . 27
Table 13 - Overall Statistics of Temperature by Pressure . . . 28
Table 14 - Interval Statistics of Humidity by Pressure 29
Table 15 - Overall Statistics of Humidity by Pressure 30
Table 16 - Overall Statistics of T_d Depression by Pressure . . 31
Table 17 - Overall Statistics of Height by Pressure 32
Table 18a - Pressure Level Statistics for Temperature 33
Table 18b - Pressure Level Statistics for Humidity 34
Table 18c - Pressure Level Statistics for Height 35

ABSTRACT

FUNCTIONAL PRECISION OF NATIONAL WEATHER SERVICE
UPPER-AIR MEASUREMENTS USING
SPACE DATA DIVISION RADIOSONDE (MODEL 909-10-01)

Test and Evaluation Branch, National Weather Service, NOAA
Sterling, Va.

The functional precision of Space Data Corporation Model 909-10-01 (SDC) radiosonde was determined using the National Weather Service functional analysis test package. The comparisons were made from 45 flights of paired radiosondes suspended from the same balloon. The two sondes were vertically separated by about 10 meters and, for this report, functional precision is given by the standard deviation of the differences (σ-D) between measurements made by 2 sensors of the same type exposed to the same environment. Results are summarized for simultaneous measurements at one minute intervals as well as measurements at a predefined set of pressure levels. These tests were conducted for the acceptance of contract production samples and results are reported here for use by the meteorological community in specifying the characteristics of this radiosonde which began operational use in February of 1989.

For comparisons made at one minute intervals, the overall functional precision for temperature was 0.3°C and ranged from 0.2 to 0.4°C. For altitudes below the 100 mb level, the precision for pressure ranged from 1.3 to 3.0 mb and 1.3 to 1.6 mb above, with an overall value of 2.1 mb. Relative humidity precision was 2%.

For comparisons made at predefined pressure levels, the functional precision for height ranged from 2 meters at 850 mb to 16 meters at 100 mb and 33 meters at 20 mb. For altitudes below 100 mb, the temperature precision ranged from 0.2 to 1.0°C and from 0.5 to 2.0°C above. Relative humidity precisions ranged from 1 to 4%.

Compared to the VIZA (Model 1492-510) time commutated sonde, precisions for data sampled at the same time for temperature and humidity were about the same and worsened for pressure. Both tests used the same automated data recording and reduction methods. Differences in performance are mainly attributed to the radiosonde design and sensor differences.

1. BACKGROUND

Functional Testing is a procedure which determines bias and variability between data sets of meteorological measurements made by two separate instruments or observation systems which are exposed to the same environment at the same time. If the data sets are provided by identical systems, the root mean square of the differences (RMSD) is a measure of variability and is termed the Functional Precision. If they are provided by dissimilar systems, the RMSD is termed Functional Comparability and the mean of the differences is the bias. For upper-air testing, the data can be compared not only at the same time but also at the same pressure. The terms and testing procedures were developed by Walt Hoehne in 1971 and functional tests on the operational NWS radiosondes were performed in 1973 and 1979 (Hoehne, 1971, 1980).

The National Weather Service (NWS) has been flying Space Data radiosondes since 1989. In 1988, the production contract for the VIZA sonde had expired and the (NWS) awarded a contract to Space Data Corporation (SDC) for the production of radiosondes for synoptic soundings at 15-20 of its U.S. stations. SDC is now Space Data Division of Orbital Sciences Corporation. At the same time, a contract was also awarded to the VIZ Manufacturing Co. for production of radiosondes for 60-65 U.S. stations.

The advantage of introducing another, independent source for radiosondes is to insure an adequate supply to continue operations if a manufacturer's production capability is lost or diminished. Also, increased competition among vendors theoretically improves cost, efficiency and product quality. A major disadvantage of a multi-sonde network is that it produces an inhomogeneous synoptic data set which, when used for model initialization, can severely degrade analyses and forecasts. Modeling techniques cannot totally compensate for this type of data anomaly. Also, changes in the radiosonde sensors and their characteristics limit the usefulness of radiosonde data for long term climatological studies. Other disadvantages include a significant increase in the test and evaluation requirements. It is necessary to determine the functional precision of a radiosonde and its comparability to any other radiosonde in concurrent or previous use.

Early in 1988, the NWS Test and Evaluation Branch within the Engineering Division of the Office of Systems Operations initiated tests in support of the new radiosonde procurement. Both replacement radiosondes were designed according to functional specifications which gave the manufacturer maximum flexibility towards meeting performance requirements. Formal acceptance of the VIZB and Space Data sondes followed successful performance testing. The VIZA sonde, introduced in 1986, was phased out by February 1989, when all conterminous U.S. and Alaskan stations had switched to the VIZB or Space Data sonde.

The radiosonde designed and built by Space Data has significant electronic and physical differences from both VIZ sondes. The major differences are in the type of temperature and pressure sensors and the exposure of the humidity sensor. The hygristor is the same as the VIZB, being provided by VIZ Manufacturing Co. However, the placement of the hygristor differs, being mounted inside a painted, "S" shaped duct for the Space Data sonde.

Functional precision testing of the VIZA and Space Data sonde, and functional comparability testing of the VIZA to the VIZB and Space Data sondes are described in separate test reports. A paper summarizing all test results was presented at the Upper-Air Measurements and Instrumentation Workshop, November 14-16, 1989, at Wallops Island, VA and at the American Meteorological Society's Seventh Symposium on Meteorological Observations and Instrumentation, January 14-18, 1991, at New Orleans, LA (Ahnert, 1991). A few differences may exist between the test results reported herein and those in the paper due to subsequent data editing for better quality control and statistical accuracy.

2. INSTRUMENT DESCRIPTION

The Space Data (Model 909-10-01) radiosonde is an expendable instrument package that is suspended below an ascending balloon. The radiosonde measures the vertical profiles of pressure (P), temperature (T), and relative humidity (U) of the atmosphere through which it ascends. These parameters are measured by sensors and the measurements are transmitted to the ground by radio. The Space Data radiosonde (Figure A1) consists of sensors, telemetry electronics, radio transmitter, and a wet-cell battery enclosed in a styrofoam case. The radiosonde physical dimensions are 4 X 8.5 X 10.5 inches and weighs 530 gm with activated battery.

The Space Data radiosonde transmits meteorological data to the ground receiving equipment using a 1680 MHz carrier wave which has been amplitude modulated into a pulse-train. The met data information is contained in the pulse repetition frequency, which may range from 100 Hz to 1 KHz and varies with the value of the parameter being measured. Each quarter second, the transmitted pulse-train is sequentially switched (time-commutated) between P, T, U, and the internal reference. The Space Data sonde repeats the same PTU data, which produces a cyclic pulse-train which represents a nominal two second sampling rate of the meteorological parameters by the radiosonde.

The pulse-train repetition frequency is controlled by sensor resistance, which varies the output of an audio frequency oscillator, referred to as the Met Data Oscillator (MDO). The sensor resistance is a function of the meteorological parameter being measured. High resistance causes the MDO to oscillate at a low frequency and visa-versa. The pulse repetition frequencies from pressure, temperature, and humidity sensors and internal reference are time-commutated in the MDO circuit (Systex, 1990).

The Space Data and VIZ radiosondes encode meteorological data in a similar manner. They modulate the frequency of an audio frequency oscillator, referred to as the Met Data Oscillator (MDO). The MDO frequency is controlled by the resistance of a sensor. This resistance is related to the value of the meteorological parameter that the sensor measures. A high resistance causes the MDO to oscillate at a low frequency and visa-versa. These resistance values, reported by the pressure, temperature, and relative humidity sensors, along with an internal reference resistance, are time commutated into the MDO circuit. The MDO amplitude modulates a 1680 MHz radio-frequency carrier wave that is transmitted to the ground receiving equipment (Systex, 1990).

The Space Data radiosonde uses a Barometric Integrated Temperature controlled Solid-state Sensor (BITSS) as its pressure sensor. BITSS is an aneroid pressure capsule which uses a silicone diaphragm with imbedded piezoresistive strain gauge. The silicone diaphragm is mounted on a thermostatically controlled pyrex substrate and packaged in a TO-5 transistor. External pressure linearly deflects the diaphragm toward the Pyrex and the amount of deflection is measured by a wheatstone bridge using the imbedded strain gauge. A heater keeps the pressure cell at a constant 55°C. Direct pressure measurements are obtained for each data frame because the BITSS produces a resistance which is a continuous function of pressure. Each pressure cell is individually calibrated by Space Data.

The temperature sensor is a ceramic chip thermistor, which has a negative thermal coefficient, produced by Victory Engineering Company (VECO). VECO calibrates the thermistor and provides three calibration coefficients to Space Data for use in an expanded linear transform equation. It is coated at Space Data with a water repellant silicone and with white lead carbonate paint to minimize the effects of solar radiations. Coated diameter is 0.095 inches. Solar and Infrared exposure of the sensor can cause positive/negative errors (Schmidlin, et. al. 1986). The thermistor is mounted on wire leads from a flexible flat plastic boom extending 5 inches from the radiosonde case.

The humidity sensor is the same carbon hygristor used in the VIZA and VIZB. It consists of a strip of plastic (2.5 X 0.7 X 0.03 inches) which has been dipped in a mixture of carbon particles dispersed in a celluloid resin and then dried. When an electric current is passed through the carbon-celluloid coating, it acts as a resistor. The celluloid is sensitive to relative humidity and expands or contracts with the amount of water vapor available. This causes a greater average distance between carbon particles and thus increases its resistance. As with temperature, each sensor for a particular lot follows a characteristic relative humidity-resistance curve family. Each hygristor is then cycled through increasing and decreasing humidity, and then scribed to produce the correct resistance at the 33% lock-in value. Due to a change in the elastic properties of the sensor materials near -40°C, the NWS does not report humidities for temperatures below that. Also, the transfer equation that is used to convert resistance to humidity is suspect at the low end and relative humidities below 20% are not reported. To simplify humidity determinations, the transfer equation uses the temperature sensed by the outboard thermistor instead of the hygristor temperature. If a there is a temperature difference between the two, the calculated RH is in error. To reduce the temperature difference by shielding the hygristor from solar effects and contact with hydrometers, it is housed inside an "S" shaped duct passing from top to bottom through the center of the styrofoam radiosonde case.

3. TEST METHODOLOGY

Data from 45 dual radiosonde flights made between December 1988 and August 1989 were used for this test. Of these, 19 were daytime, and 26 were nighttime releases. The initial operational version of the Space Data radiosonde and software were used. A dual flight consisted of two Space Data radiosondes suspended from one balloon. All flights for this test were made at the Sterling Research and Development Center, Sterling, VA located 20 miles west of Washington, D.C..

3.1 RADIOSONDE PREPARATION/RELEASE

A 600 gram or larger balloon was prepared and filled with hydrogen gas to a nozzle lift of 2400-2900 grams. The balloon train included 2 parachutes and terminated with the two Space Data sondes vertically separated by 30 feet. Earlier versions of the SDD radiosonde were found to be sensitive to frequency interference from other sondes when space horizontally. Later testing has revealed that the frequency sensitivity problems have been corrected. The train length ranged from 120 feet, for release in low wind speeds, to 50 feet, for release in strong winds.

Both Space Data radiosondes were prepared and released according to standard NWS operating procedures (NWS, 1981). The transmitter frequencies were adjusted so that the separation was at least 10 MHz. All radiosondes used for these tests passed a baseline test requiring that the sonde measured pressure be within ±5.0 mb of station pressure.

All of the flights were performed after dual remote control units were installed at the release site. This, combined with a radio triggered release switch, allowed for 1 person releases in low surface winds and 2 person releases otherwise.

3.2 GROUND EQUIPMENT

The ground equipment consisted of two ART systems and minicomputers, designated ART-1R and ART-2R. Both system configurations were identical to operational NWS equipment. The ART-1R uses a GMD type radiotheodolite and the ART-2R uses a WBRT type radiotheodolite. Most of the electronics are solid state. Differences between the systems occasionally result in differences in signal strength and noise levels but will not induce any biases in the pressure, temperature, and humidity data. Since wind data characteristics are primarily a function of the ground equipment and not the radiosonde, they were not analyzed as a part of this test.

3.3 DATA REDUCTION

The Space Data sonde uses a 1680 MHz carrier wave to cyclically transmit the sensor data, as a pulse-train, at a nominal rate of once per second. The cycle's (i.e., data frame) sequence corresponds to sensed pressure (P), temperature (T), relative humidity (U), and high or low reference values. The pulse-train for each parameter is transmitted for a quarter of the cycle and is referred to as the data sub-frame for that parameter. For each sub-frame, the sensor resistance, which corresponds to the parameter's value, determines a pulse repetition frequency between 100 and 1 KHz. During the sub-frame transmission, the MDO modulates the amplitude of the carrier wave so that it is large for a period which corresponds to the correct pulse repetition frequency for the value of the met parameter. The radiosonde signal is then received and automatically tracked by the radiotheodolite's parabolic antenna. The ART receiver amplifies the subframe signal to 0.5 volts. The pulse-train signal is sent to the ART Interface Board (ARTIB) located in the minicomputer. For each sub-frame, the ARTIB measures the time of arrival for each pulse and interrupts the minicomputer.

Using the ARTIB generated interrupts, the minicomputer software synchronizes with the radiosonde commutation cycle, computes average period values for reference and each data subframe, and stores the data. After synchronization, the data is filtered, using a histogram technique. This separates the dominant frequency from the noise and assigns a data quality indicator for each parameter subframe. From the sub-frame data, an average value for a six second interval is calculated for pressure, temperature, relative humidity, and reference frequencies. This produces a data set with an effective 0.1 minute sampling rate. The frequency data form the data set stored on the minicomputer system tape.

Although the minicomputer continues on to select mandatory and significant levels and compose messages, that information was not used for these tests. Following each flight the 6 second frequency data were transferred from the system tape to a second log tape. Then the microcomputer was booted from a special system tape and a program run to dump the data from the log tape to a microcomputer at 2400 bps. The microcomputer then dumped the data to a floppy disk.

The data reduction was done on the microcomputer. Surface and radiosonde administrative data were entered. The microcomputer processed the 6 second frequency data into meteorological units of pressure (mb), temperature (C), relative humidity (%), and height (m). From this 6 second met data, one minute and mandatory level data were extracted, put into the "RAWIN.DAT" file and written to floppy disk.

The one minute data were obtained by extracting the met data from the 6 second data period which contained the whole minute. If the met data value was missing for the 6 second data, it was also reported as missing for the one minute data (i.e., no interpolation was performed).

The mandatory level data were obtained from the 6 second frequency data by first interpolating, to the nearest 0.06 second, the time when the radiosonde reached the mandatory pressure. Then interpolations were performed using the 6 second frequency data bracketing the mandatory level. If either of the 6 second values was missing the mandatory level value was also reported as missing.

The two floppy disks containing the RAWIN.DAT files for the two radiosondes flown were then clearly identified and catalogued. When time permitted, the dual flight data were loaded into the Functional Analyses Testing Package (FATP). This software package runs on a 80286 microcomputer and consists of off-the-shelf database, statistics, and graphics software. These have been integrated with customized software to perform functional analyses of dual radiosonde data. After entering the data from each flight, it was plotted and reviewed. All statistics, tables and figures contained herein were produced by the FATP.

For the computation of the root mean square of the differences (RMSD), the number of samples, N, was used. For the computations of standard deviation of the differences (σ-D), N-1 was used. As a result, for cases of small N (less than 100), some of the computed σ-D's are larger than the corresponding RMSD. For consistency, N-1 should have been used for both. However, the effect of such a change on the reported results would be insignificant. If desired, they can be adjusted by multiplying the reported RMSD by $1.0 + 0.5/N$ (note: this correction is valid for N greater than or equal to 10). It can be seen that, for N=10, the difference is 5 percent, for N=50 it is 1 percent, and for N=100 it is 0.5 percent. For N greater than 100 the correction is very small. When N is less than 100, due to the limited sample size, the RMSD and σ-D are only rough estimates.

4. COMPARISON BY TIME

The time comparisons for pressure, temperature, relative humidity and dew-point depressions were made using the one minute data. One minute heights were extracted from heights calculated from the 6 second data. If that height was missing, no interpolation was performed. Since radiosondes were separated 30 feet vertically, they were sampling slightly different conditions at the same time. Given the nominal ascension rate of 5 meters per second, the bottom sonde reached any height approximately 2 seconds after the top sonde. The effect on the statistics depends on how much variation occurs in those 2 seconds (10 meters) and whether the cumulative variations are systematic or random. The Functional Analyses Testing Package (FATP) computed simultaneous differences between the two sondes (i.e., top minus bottom) for pressure, temperature, relative humidity, dew-point depression, and height for each minute of flight. The root mean square of the differences (RMSD) was used to determine the radiosonde's functional precision for that parameter. However, if systematic biases (mean differences) are attributable to the vertical separation, then the standard deviation is used. This eliminates the effects of systematic biases on the functional precision (Hoehne, 1980). The kurtoisis (flatness) for a normal distribution has a value of 3.0.

Histograms, frequency tables, scatter plots and linear regressions were also generated using the FATP software. Where possible the measurement range was divided into intervals and the functional precision for each interval was computed. This can provide insight on the variability of performance over the measurement range. For pressure, temperature, and relative humidity, precision was also computed for intervals of pressure corresponding to analyses done during the World Meteorological Organization (WMO) international radiosonde intercomparisons.

4.1 PRESSURE

For the total population, 84.8% of pressure differences by time were between ±2.0 mb, 64.8% were between ±1.0 mb and 02.1% exceeded ±3.0 mb (Figure 1, Table 1). The relative frequencies for the magnitude of pressure difference occurring within a difference interval are given for 7 pressure layers (Table 1).

The scatter plot (Figure 2) shows a number of points from flight #383 where secondary pressures exceeded primary pressures by up to 14.2 mb. Figure A-2 shows the pressure difference for each minute of flight #383 and indicates that one or both radiosondes had large pressure errors.

Because of the 30 foot vertical separation between radiosondes, the standard deviation of the differences (σ-D) is used to indicate functional precision. However, the differences between root mean square of the differences (RMSD) and the σ-D are very small.

The overall functional precision (σ-D) for pressure by time is 2.1 mb. For the 7 pressure layers, precisions ranged from 1.3 mb between 50 and 100 mb, to 2.4 mb between 100 and 500 mb (Table 1). A table and graph with precisions for 14 pressure intervals used in the WMO intercomparisons are also included (Figure 3, Table 3).

The overall functional precision of the Space Data sonde for pressure by time is 0.8 mb worse than the VIZA used by NWS from 1986-1989 (Ahnert, 1990b) and 0.2 mb worse than the VIZ Pressure Commutated radiosonde tested in 1980 (Hoehne, 1980). This precision slightly exceeds the ±2.0 mb tolerance of the current specification, however, it would have to exceed ±2.2 mb before the σ-D would be statistically significant.

The mean pressure differences (bias) of -0.9 mb from 850 to 1010 mb and -0.7 mb from 500 to 850 mb closely match the expected bias caused by the 30 foot vertical separation. As expected, above this level, the differences become smaller and are not significantly different from 0. The significance criteria used is from section 3.2 of Hoehne (1977) with the assumption that for one minute pressure data the number of independent samples is $n = N/4$.

Recent tests revealed that a gel coating used on the pressure cell was hygroscopic. Absorption of water vapor by the gel caused long-term calibration drifts in the baseline pressure. During a flight, the sensor is heated to 55°C and tends to purge the absorbed water from the gel. This process affects the sensed pressure in the following way. The difference between the factory calibrated pressure and that measured during the preflight baseline procedure is used as a percentage to correct pressures throughout the flight. As the gel is purged of water during the flight, the pressure cell should recover to its factory calibration and the applied baseline pressure correction would be no longer applicable. Also, the corrections applied to both sondes would affect the statistics by guaranteeing a constant pressure difference percentage between the two sondes for the whole flight. In summer 1989, Space Data began sealing the BITSS with tape that was removed before the sonde was used. In spring 1990, a further modification was made which bypasses the hygroscopic problem by eliminating the gel coating as well as taping the BITTS during shipment/storage.

4.2 TEMPERATURE

For the total population, 93% of the temperature differences by time were ±0.5°C or less (Figure 4, Table 4). The relative frequencies for the magnitude of temperature difference occurring within a difference interval are given for 7 temperature intervals (Table 4).

The scatter plot (Figure 5) shows increasing scatter at lower temperatures and some anomalous points belonging to flight #383 (Figure A-2). For flight #383, differences up to 6°C occurred for 5 minutes.

The overall functional precision (σ-D) for temperature by time is 0.33°C (Table 4). For the 7 temperature intervals, precisions ranged from 0.23°C between -20 and -5°C, to 0.33°C between -90 and -60°C. Due to the small sample size (42), the 0.71°C precision for warm temperatures should be used with caution. However, because of the vertical radiosonde separation and large lapse rates near the surface on summer days, it would be expected to be worse for warm surface conditions than for cooler. Precisions of temperature for 15 pressure intervals used in the WMO intercomparisons are given in Figure 6 and Table 6.

Overall functional precision of the Space Data radiosonde for temperature compared by time is nearly the same as the 0.34°C found for the VIZA (Ahnert, 1990b). This is well within the 0.5°C tolerance of the current specifications.

Mean difference (Bias) for 7 ranges of temperature are given in Table 4. They ranged from +0.09°C to -0.04°C. A small negative bias is expected in the troposphere, where the temperature decreases with height combines with the 10 meter vertical separation between radiosondes. The opposite is expected in the stratosphere, where the temperature increases with height. This is shown in the data. The anomalous bias of +0.09 (top sonde warmer) between 20 and 35°C is not reliable due to the small sample size (42 cases).

The stratospheric bias reversal is evident in the data given Tables 4 and 6, and Figure 6. For the temperature interval from -90 to -60°C, the 0.08°C size of the positive bias (i.e, top sonde warmer than bottom sonde) is surprising. Based on the number of independent samples (548/4=137), it is statistically significant.

A possible explanation is the difference in radiative transfer between the sonde thermistors and the balloon (Tiefenau and Gebbeken, 1989) or temperature wakes caused by the balloon (Ney, et. al 1961). At 20 mb, a balloon can expand to a 20 foot diameter. For a normal release, the balloon is normally 100 feet from the top sonde and 130 feet from the bottom sonde. For a release in high surface winds, it would be only 50 and 80 feet away from them. In the tropopause, the sounding would be between warmer parts of the atmosphere and both solar and infrared effects would be important. Upward and downward infrared radiation would tend to heat the balloon relative to the ambient air. Infrared energy could be transferred from the enlarged balloon to the thermistors. In addition to this, the balloon would warm air flowing around it, leaving a laminar temperature wake which the radiosondes might encounter at different times.

Despite all the interesting potential effects caused by the vertical separation and balloon, the biases are less than the resolution of the temperature measurement and the functional precision values taken from the standard deviation or root mean square of the differences are virtually identical.

4.3 HUMIDITY

Relative humidity is measured by the radiosonde hygristor in terms of electrical resistance. It is converted to dew-point depressions for message coding and transmission to other users. To determine a measure of humidity from the dew-point depression, the temperature must be known, so, if the temperatures reported by both sondes used in the comparisons are not the same, the dew-point depression differences do not give a pure measure of the humidity statistics but rather a combined measure of temperature and humidity statistics which are difficult to objectively analyze.

4.3.1 RELATIVE HUMIDITY

For the total population, 98.2% of the Relative Humidity differences by time were 5% RH or less (Table 7). Relative frequencies of the magnitude of relative humidity differences occurring within a difference range are given for 10 humidity intervals (Table 7).

The scatter plot (Figure 8) shows a large amount of variance throughout the humidity range. The largest relative humidity difference was 40.6% RH (Table 8).

Overall functional precision (σ-D) of relative humidity by time is 2.2% RH (Figure 7, Table 7). For the 10 relative humidity intervals, precisions ranged from 1.50% between 70 and 80% RH to 2.72% between 10 and 20% RH. Precisions for 5 pressure intervals used in the WMO intercomparison tests are presented in Figure 9 and Table 9.

Except for the first WMO pressure interval, the data given in Figure and Table 9 reveal a slight trend of worsening precision with decreasing pressure. The 2.9% RH precision for the first pressure interval was calculated from a small sample size (55) and should be used with caution. This interval also includes effects caused by preflight variations in exposure or poor initial flight ventilation.

The overall functional precision of the Space Data sonde for relative humidity by time was 0.1% worse (larger σ-D) than the 2.1% RH found for the VIZA (Ahnert, 1990b). The precision was within the 5.0% RH tolerance for the current specification.

Except for the -0.88% RH mean difference of the 40 and 50% RH interval, the biases were small and ranged from -0.54% to 0.34%. Based on the number of independent samples (134), the -0.88% value is significant (Hoehne 1980). This large negative bias may be accounted for by the vertically separated sondes exiting cloud layers with the top sonde reporting the lower humidities first. The differences can be large and will be negatively biased. The humidity v. time plot for flight #291 (Figure A-4) shows this at minute 9, where a difference of about -15% RH is recorded. A less possible cause is the lower sonde swinging through the vapor wake from the top sonde's wet-cell battery. In contrast to mean differences (bias), which are largest in the middle of the measurement range, the greatest scatter (variance) occurs at low and high humidities (Figure 8).

The standard NWS 20% humidity cutoff was not applied to these data since it would have caused considerable problems with the statistics. Please note, however, that the accuracy of humidities below 20% calculated using current NWS equations is questionable so indicated precisions at these humidities may not reflect a trend in precision for the measurement range.

4.3.1 DEW-POINT DEPRESSION

The overall functional precision (σ-D) of dew-point depression by time is 2.8°C (Table 10). This is 0.7°C better than the VIZA (Ahnert, 1990b) and the 0.9°C better than the VIZ pressure-commutated radiosonde (Hoehne, 1980).

Unfortunately, statistics computed in these and Hoehne's tests are affected by the NWS practice of reporting a 30°C dew-point depressions 20% RH or lower. This affects the statistics in the following two ways. First, when both sondes are measuring 20% RH or less, both get assigned depressions of 30°C, and a false number of cases indicating no differences are used in the statistics. Secondly, if one sonde measures slightly above 20% RH and the other measure 20% RH or less, an artificially large difference value is used in the statistics. The large differences are visible in the histogram of dew-point depression differences (Figure 10). These two effects tend to cancel each other out to some extent but it is not known whether the net effect is to increase or decrease the estimated functional precision.

4.5 HEIGHT

The overall functional precision (σ-D) for height by time is 231 meters (Figure 11, Table 11). This is 128 meters worse (larger σ-D) than the VIZA sonde (Ahnert, 1990b). This figure should be used with caution since a larger number of high altitude flights were included in the Space Data sample and the effect of the 10 meter vertical separation was not removed.

Note that, except for winds, data versus heights obtained at the same time are seldom used in meteorological analyses. Height measurements of pressure levels are discussed in section 5.3.

Comparing the magnitude of height differences with height produced a strong correlation of 0.48 (i.e., more height scatter at greater heights).

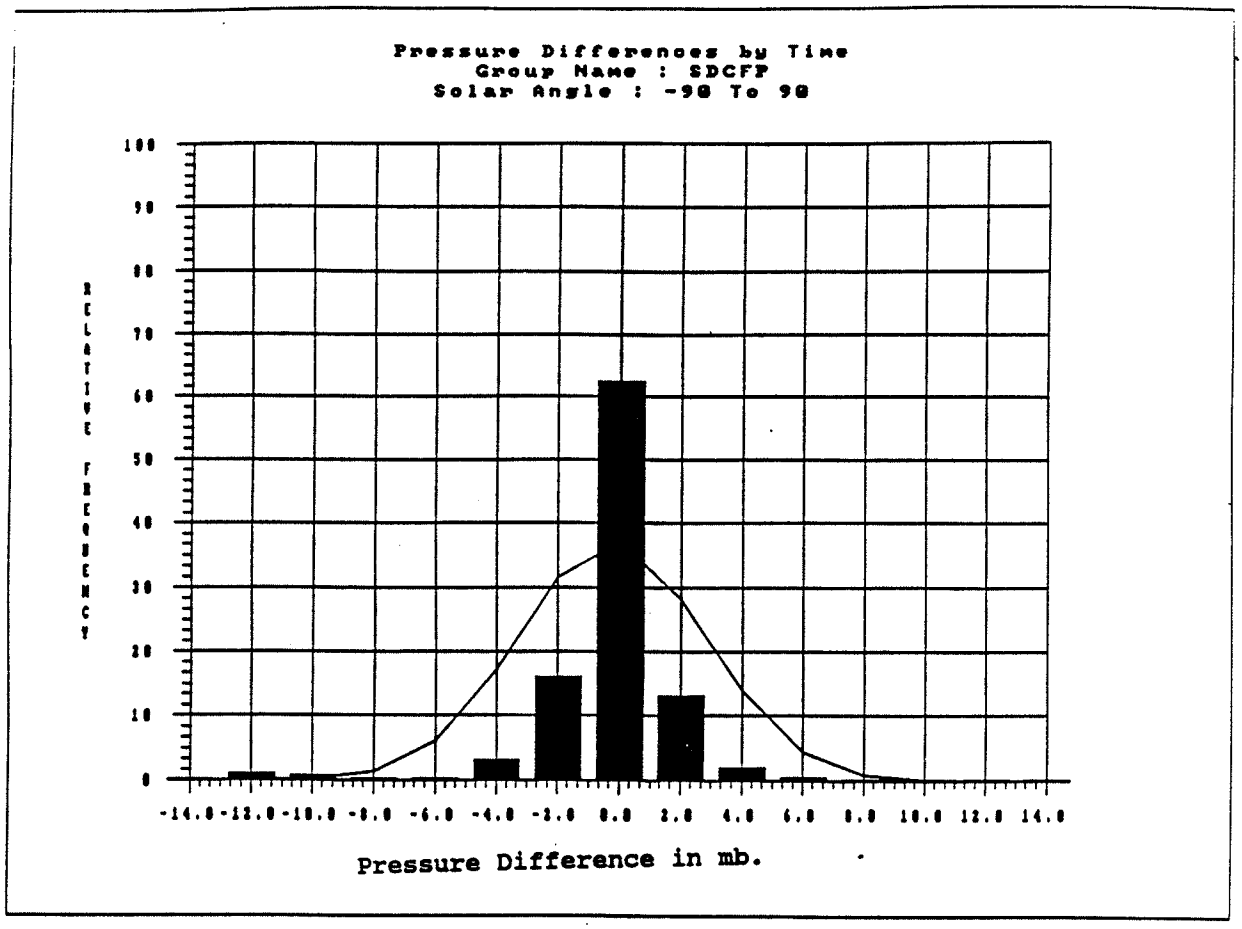

Figure 1. Histogram of Pressure Difference sampled at same time of flight Normal curve computed from sample mean and standard deviation.

MB. FROM	TO	SAMPLE SIZE	# OF FLIGHTS	Absolute Pressure Difference Interval 0.0-0.5	0.6-1.0	1.1-1.5	1.6-2.0	2.1-2.5	2.6-3.0	> = 3.1	MEAN DIFF.	RMS DIFF.	STD.DEV. DIFF.
				Relative Frequency in %.									
1010.0	THRU 1050.0	7	7	100.0	0.0	0.0	0.0	0.0	0.0	0.0			
850.0	THRU 1009.9	240	45	36.7	15.8	17.1	12.1	7.9	4.2	6.3	-.92	2.39	2.21
500.0	THRU 849.9	696	45	37.1	24.3	15.4	8.6	4.3	2.6	7.8	-.68	2.37	2.27
100.0	THRU 499.9	1607	44	40.2	24.4	12.3	8.3	4.5	1.5	8.7	-.31	2.40	2.38
50.0	THRU 99.9	430	34	39.5	27.9	14.4	6.0	4.7	1.2	6.3	.28	1.32	1.29
20.0	THRU 49.9	383	26	44.1	28.2	7.0	3.1	6.3	2.6	8.6	.30	1.45	1.42
0.0	THRU 19.9	208	20	47.6	24.5	8.2	0.0	7.2	3.8	8.7	.33	1.57	1.54
	ALL	3571	45	40.2	24.6	12.7	7.3	5.1	2.1	8.0	-.25	2.16	2.14

Table 1. Frequency of occurrence (%) of Absolute Pressure Difference within selected pressure layers and for all data. Mean, rms (functional precision), and std. dev. of Pressure Difference for layers and all data. Sampled at same time of flight.

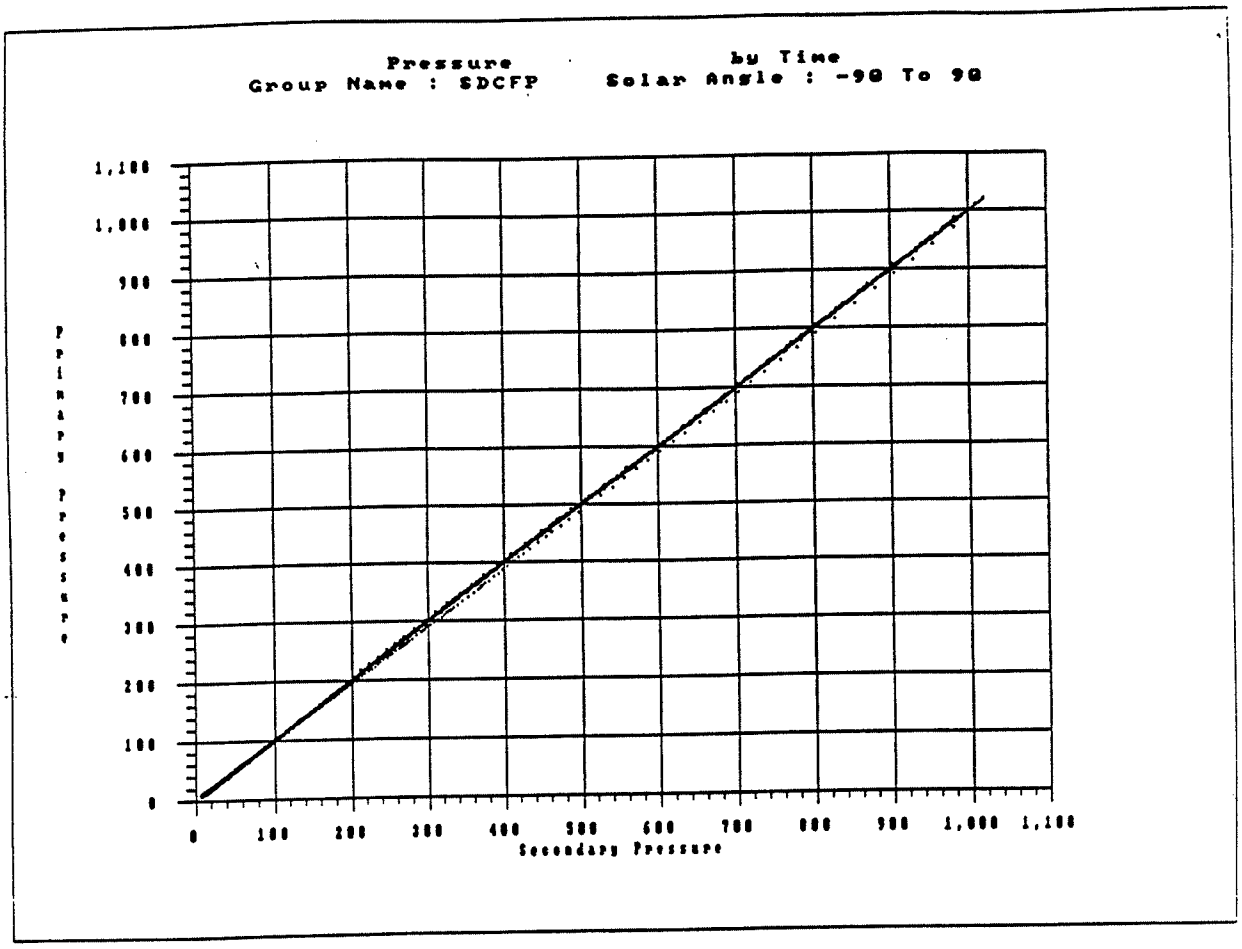

Figure 2. Scatter plot of 'primary sonde' Pressure versus 'secondary sonde' Pressure sampled at same time of flight. Regression line also plotted.

SAMPLE SIZE	# OF FLIGHTS	MEAN DIFF	STD DEV DIFF	RMS DIFF	SKEW. DIFF	KURT. DIFF	CORR. P & S	PRIM MIN	PRIM MAX	SECOND MIN	SECOND MAX	DIFFER MIN	DIFFER MAX
3571.0	45	-.25	2.14	2.16	-2.56	15.60	1.00	7.70	1020.00	5.90	1020.00	-14.20	7.20

Table 2. Pressure sampled at same time of flight. Mean, std. dev., rms, skewness, and kurtosis of differences. 'Primary sonde' and 'secondary sonde' correlation. Minimum and maximum Pressure and Pressure Difference in mb.

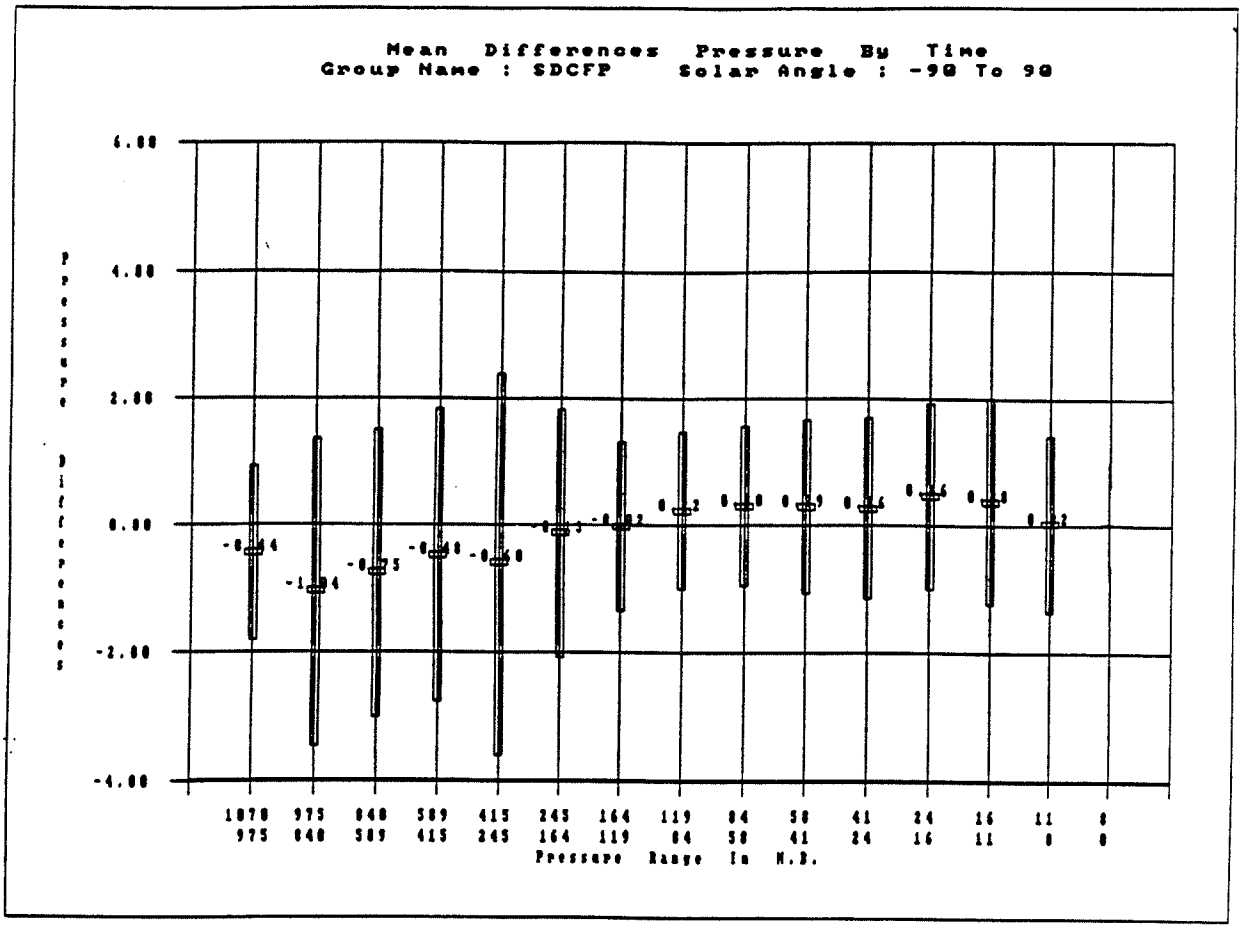

Figure 3. Mean/std. deviation of Pressure Difference within selected pressure layers. Plotted values are mean differences (mb). Bar gives +/- 1 std. deviation. Sampled at same time of flight.

FROM	MB.	TO	SAMPLE SIZE	# OF FLIGHTS	PRIMARY MEAN	SECONDARY MEAN	MEAN DIFF	RMS DIFF	STD DIFF
975.0	THRU	1069.9	55	35	991.99	992.43	-.44	1.43	1.38
840.0	THRU	974.9	215	45	902.32	903.36	-1.04	2.64	2.43
589.0	THRU	839.9	469	44	705.91	706.66	-.75	2.39	2.27
415.0	THRU	588.9	421	44	497.78	498.26	-.48	2.36	2.32
245.0	THRU	414.9	610	44	323.09	323.69	-.60	3.06	3.00
164.0	THRU	244.9	394	42	202.06	202.19	-.13	1.96	1.96
119.0	THRU	163.9	257	36	140.72	140.74	-.02	1.34	1.34
84.0	THRU	118.9	250	34	100.99	100.77	.22	1.26	1.25
58.9	THRU	83.9	216	32	71.01	70.72	.30	1.31	1.28
41.5	THRU	58.8	182	29	49.90	49.61	.29	1.40	1.38
24.5	THRU	41.4	220	24	32.36	32.09	.26	1.45	1.43
16.4	THRU	24.4	140	22	20.34	19.88	.46	1.54	1.48
11.9	THRU	16.3	93	19	14.16	13.78	.38	1.67	1.63
8.4	THRU	11.8	44	12	10.38	10.36	.02	1.39	1.40

Table 3. Mean, rms (functional precision), and std. dev. of Pressure Difference within selected pressure layers. Sampled at same time of flight.

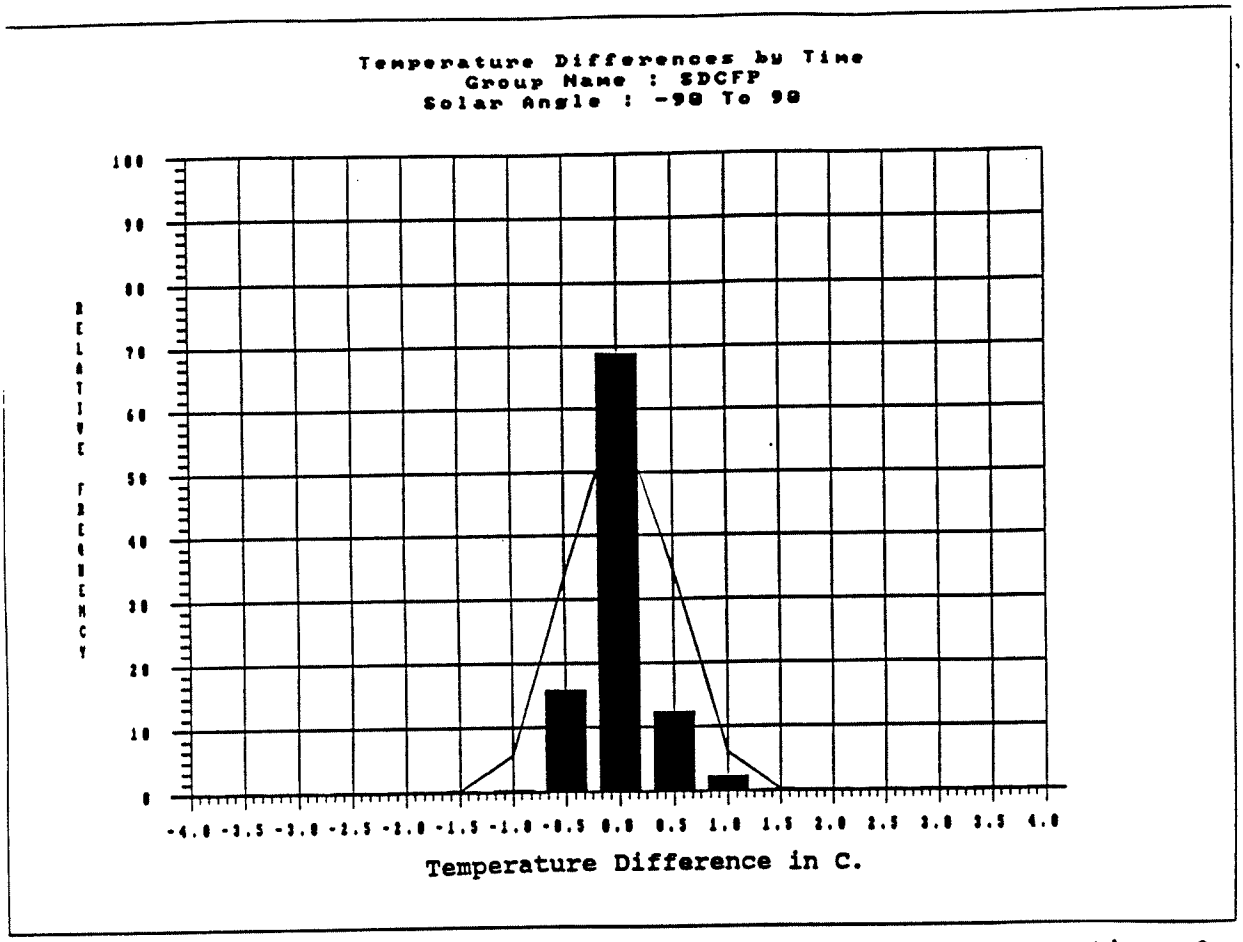

Figure 4. Histogram of Temperature Difference sampled at same time of flight. Normal curve computed from sample mean and std. dev.

DEG. FROM		DEG. TO	SAMPLE SIZE	# OF FLIGHTS	Absolute Temperature Difference Interval 0.0-0.5	0.6-1.0	1.1-1.5	1.6-2.0	2.1-2.5	2.6-3.0	> = 3.1	MEAN DIFF.	RMS DIFF.	STD.DEV. DIFF.
					Relative Frequency in %.									
20.0	THRU	34.9	42	13	83.3	14.3	0.0	0.0	0.0	0.0	2.4	.09	.71	.71
5.0	THRU	19.9	256	33	93.8	5.9	.4	0.0	0.0	0.0	0.0	-.01	.30	.30
-5.0	THRU	4.9	322	39	95.7	4.0	.3	0.0	0.0	0.0	0.0	-.02	.25	.25
-20.0	THRU	-5.1	426	44	96.9	3.1	0.0	0.0	0.0	0.0	0.0	-.04	.23	.23
-40.0	THRU	-20.1	552	44	94.7	4.3	.4	0.0	0.0	.2	.4	-.03	.40	.40
-60.0	THRU	-40.1	1425	44	90.8	8.6	.5	.1	0.0	0.0	0.0	.01	.32	.32
-90.0	THRU	-60.1	548	39	90.0	9.1	.7	.2	0.0	0.0	0.0	.08	.34	.33
	ALL		3571	45	92.6	6.8	.4	.1	0.0	.0	.1	.01	.33	.33

Table 4. Frequency of occurrence (%) of Absolute Temperature Difference within selected temperature intervals and for all data. Mean, rms (functional precision), and std. dev. of Temperature Difference for intervals and all data. Sampled at same time of flight.

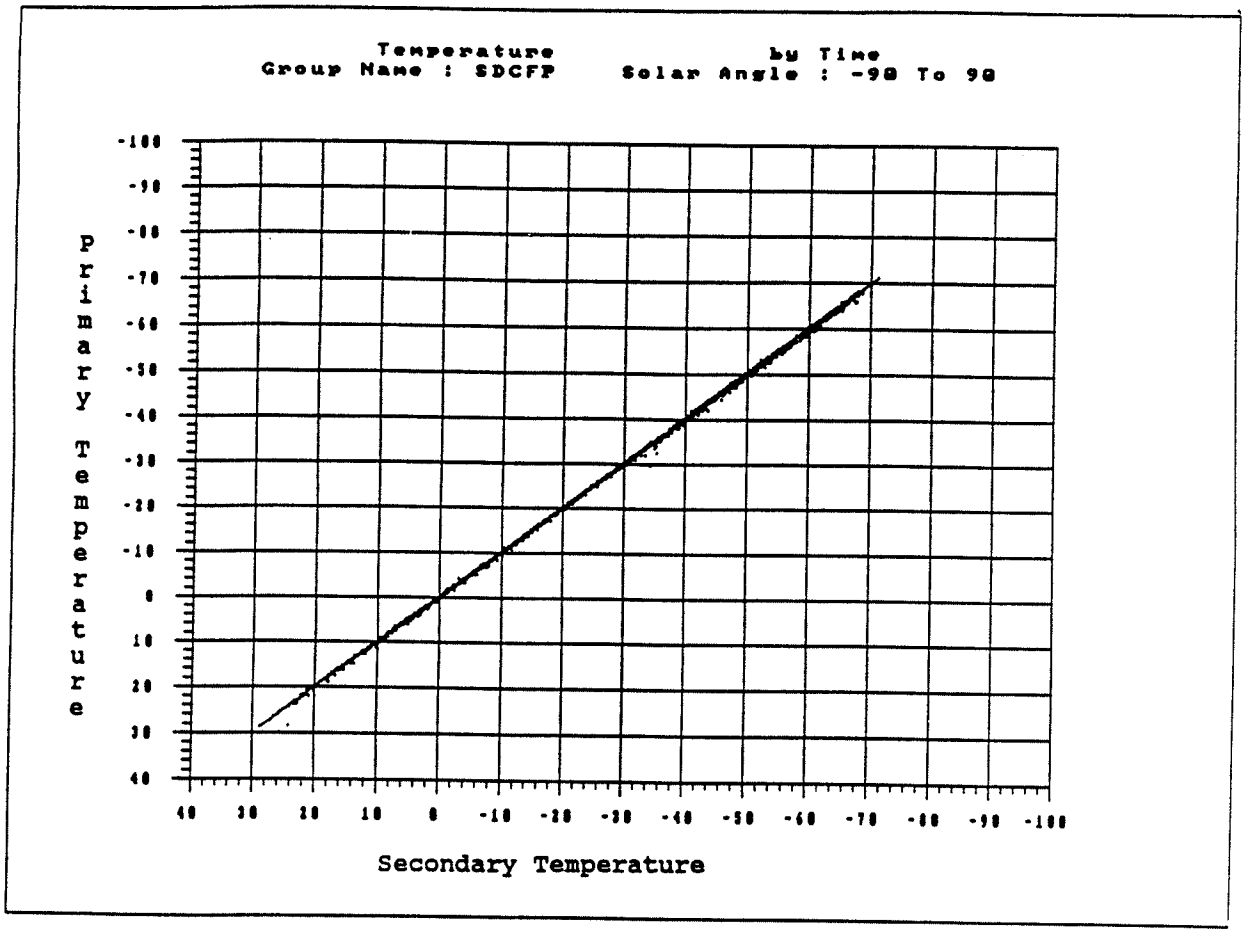

Figure 5. Scatter plot of 'primary sonde' Temperature versus 'secondary sonde' Temperature sampled at same time of flight. Regression line also plotted.

SAMPLE SIZE	# OF FLIGHTS	MEAN DIFF	STD DEV DIFF	RMS DIFF	SKEW. DIFF	KURT. DIFF	CORR. P & S	PRIM MIN	PRIM MAX	SECOND MIN	SECOND MAX	DIFFER MIN	DIFFER MAX
3571.0	45	.01	.33	.33	2.85	34.45	1.00	-71.10	28.60	-71.20	28.80	-1.20	4.80

Table 5. Temperature sampled at same time of flight. Mean, std. dev., rms, skewness, and kurtosis of differences. 'Primary sonde' and 'secondary sonde' correlation. Minimum and maximum Temperature and Temperature Difference in degrees C.

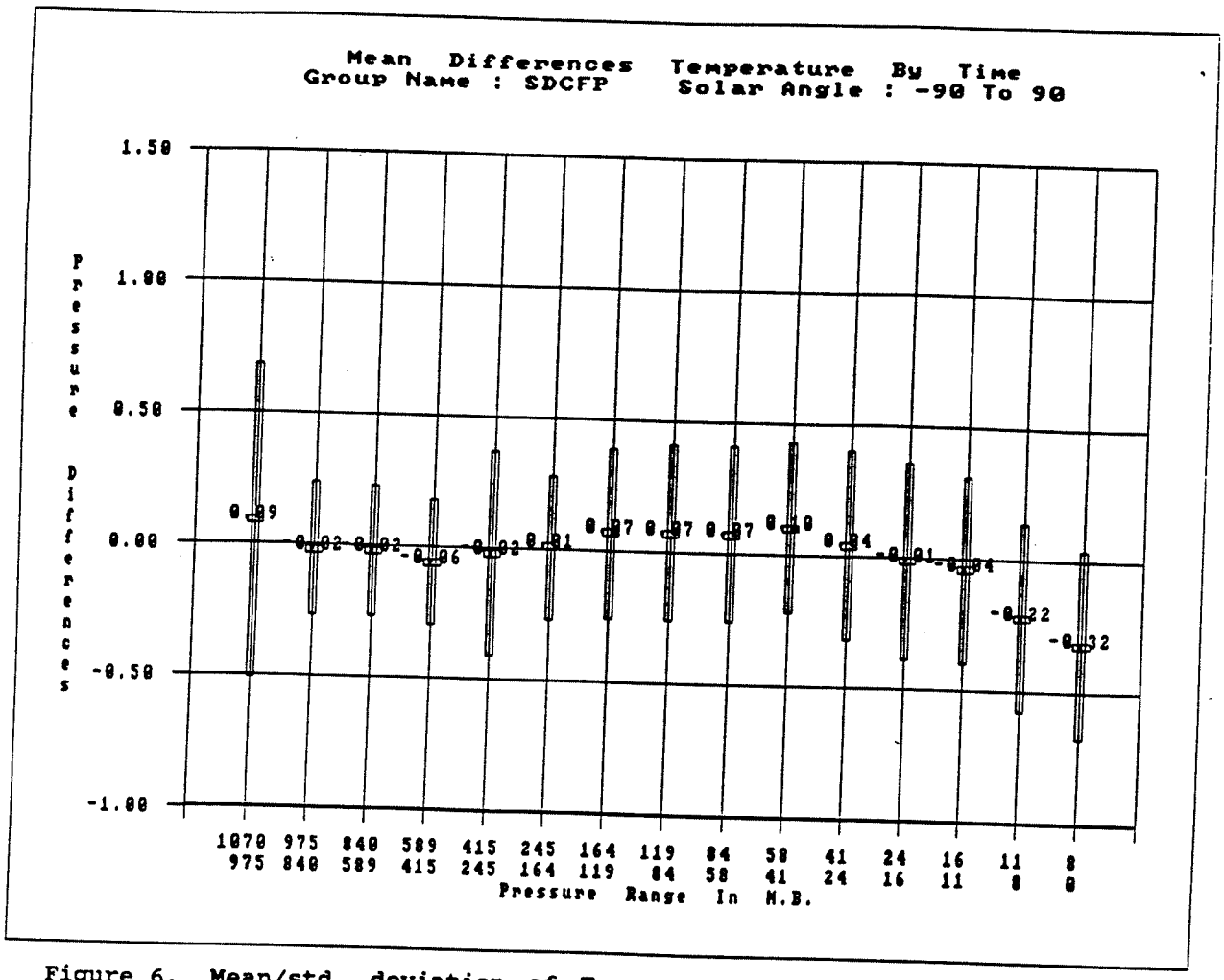

Figure 6. Mean/std. deviation of Temperature Difference within selected pressure layers. Plotted values are mean differences (deg. C). Bar gives +/- 1 std. deviation. Sampled at same time of flight.

FROM	MB.	TO	SAMPLE SIZE	# OF FLIGHTS	PRIMARY MEAN	SECONDARY MEAN	MEAN DIFF	RMS DIFF	STD DIFF
975.0	THRU	1069.9	55	35	12.36	12.27	.09	.60	.60
840.0	THRU	974.9	215	45	8.25	8.27	-.02	.26	.26
589.0	THRU	839.9	469	44	-.73	-.71	-.02	.25	.25
415.0	THRU	588.9	421	44	-15.50	-15.44	-.06	.24	.24
245.0	THRU	414.9	610	44	-37.07	-37.06	-.02	.39	.39
164.0	THRU	244.9	394	42	-54.80	-54.81	.01	.27	.27
119.0	THRU	163.9	257	36	-60.07	-60.13	.07	.33	.32
84.0	THRU	118.9	250	34	-62.44	-62.51	.07	.34	.33
58.9	THRU	83.9	216	32	-60.83	-60.91	.07	.34	.34
41.5	THRU	58.8	182	29	-56.90	-57.00	.10	.34	.32
24.5	THRU	41.4	220	24	-52.96	-53.00	.04	.37	.36
16.4	THRU	24.4	140	22	-47.14	-47.13	-.01	.37	.37
11.9	THRU	16.3	93	19	-42.21	-42.17	-.04	.36	.36
8.4	THRU	11.8	44	12	-38.53	-38.31	-.22	.42	.36
0.0	THRU	8.3	5	4	-37.66	-37.34	-.32	.45	.36

Table 6. Mean, rms (functional precision), and std. dev. of Temperature Difference within selected pressure layers. Sampled at same time of flight.

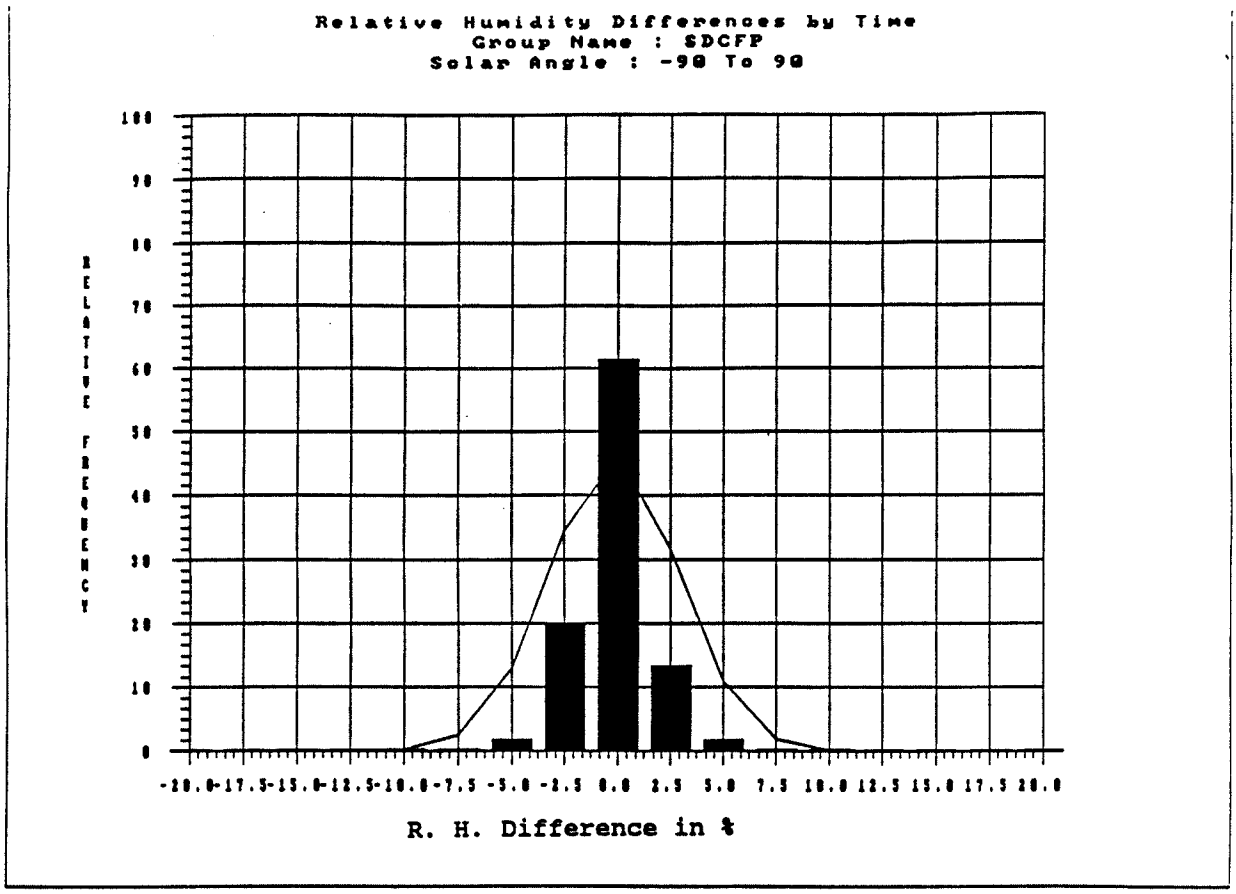

Figure 7. Histogram of Relative Humidity Difference sampled at same time of flight. Normal curve computed from sample mean and std. dev.

FROM	PERC	TO	SAMPLE SIZE	# OF FLIGHTS	Absolute R. H. Difference Interval 0.0-2.5	2.6-5.0	5.1-7.5	7.6-10.0	10.1-12.5	12.6-15.0	> = 15.1	MEAN DIFF.	RMS DIFF.	STD.DEV. DIFF.
					Relative Frequency in %									
90.0	THRU	100.0	228	28	90.8	7.5	.9	.4	.4	0.0	0.0	.34	1.71	1.68
80.0	THRU	89.9	143	35	90.9	4.9	1.4	2.1	.7	0.0	0.0	-.10	2.06	2.06
70.0	THRU	79.9	148	35	90.5	9.5	0.0	0.0	0.0	0.0	0.0	-.45	1.56	1.50
60.0	THRU	69.9	121	37	89.3	9.1	0.0	.8	0.0	.8	0.0	-.51	2.15	2.09
50.0	THRU	59.9	89	34	75.3	23.6	1.1	0.0	0.0	0.0	0.0	-.54	2.11	2.05
40.0	THRU	49.9	132	32	81.1	18.2	.8	0.0	0.0	0.0	0.0	-.88	2.02	1.83
30.0	THRU	39.9	168	33	93.5	6.0	0.0	.6	0.0	0.0	0.0	-.21	1.54	1.53
20.0	THRU	29.9	257	34	77.8	18.3	2.7	0.0	.8	.4	0.0	.32	2.46	2.44
10.0	THRU	19.9	305	25	95.4	3.0	.7	.7	0.0	0.0	.3	-.12	2.71	2.72
00.0	THRU	09.9	7	1	0.0	100.0	0.0	0.0	0.0	0.0	0.0			
	ALL		1598	45	87.7	10.5	.9	.5	.3	.1	.1	-.16	2.16	2.15

Table 7. Frequency of occurrence (%) of Absolute Relative Humidity Difference within selected relative humidity intervals and for all data. Mean, rms (functional precision), and std. dev. of Relative Humidity Difference for layers and all data. Sampled at same time of flight.

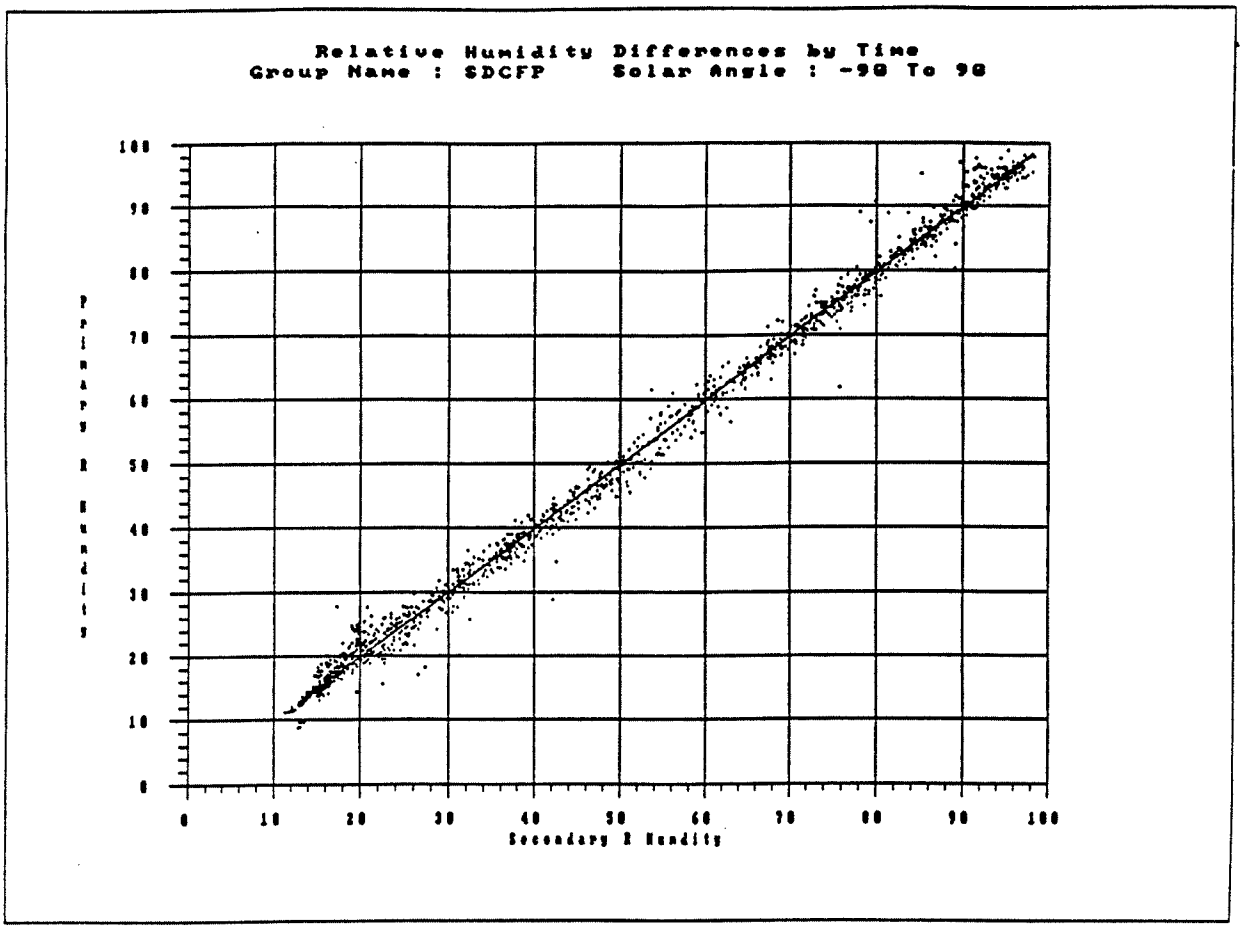

Figure 8. Scatter plot of 'primary sonde' Relative Humidity versus 'secondary sonde' Relative Humidity sampled at same time of flight. Regression line also plotted.

SAMPLE SIZE	# OF FLIGHTS	MEAN DIFF	STD DEV DIFF	RMS DIFF	SKEW. DIFF	KURT. DIFF	CORR. P & S	PRIM MIN	PRIM MAX	SECOND MIN	SECOND MAX	DIFFER MIN	DIFFER MAX
1598.0	45	-.16	2.15	2.16	4.21	87.38	1.00	8.80	98.90	11.30	98.30	-13.90	40.60

Table 8. Relative Humidity sampled at same time of flight. Mean, std. dev., rms, skewness, and kurtosis of differences. 'Primary sonde' and 'secondary sonde' correlation. Minimum and maximum Relative Humidity Difference in percent.

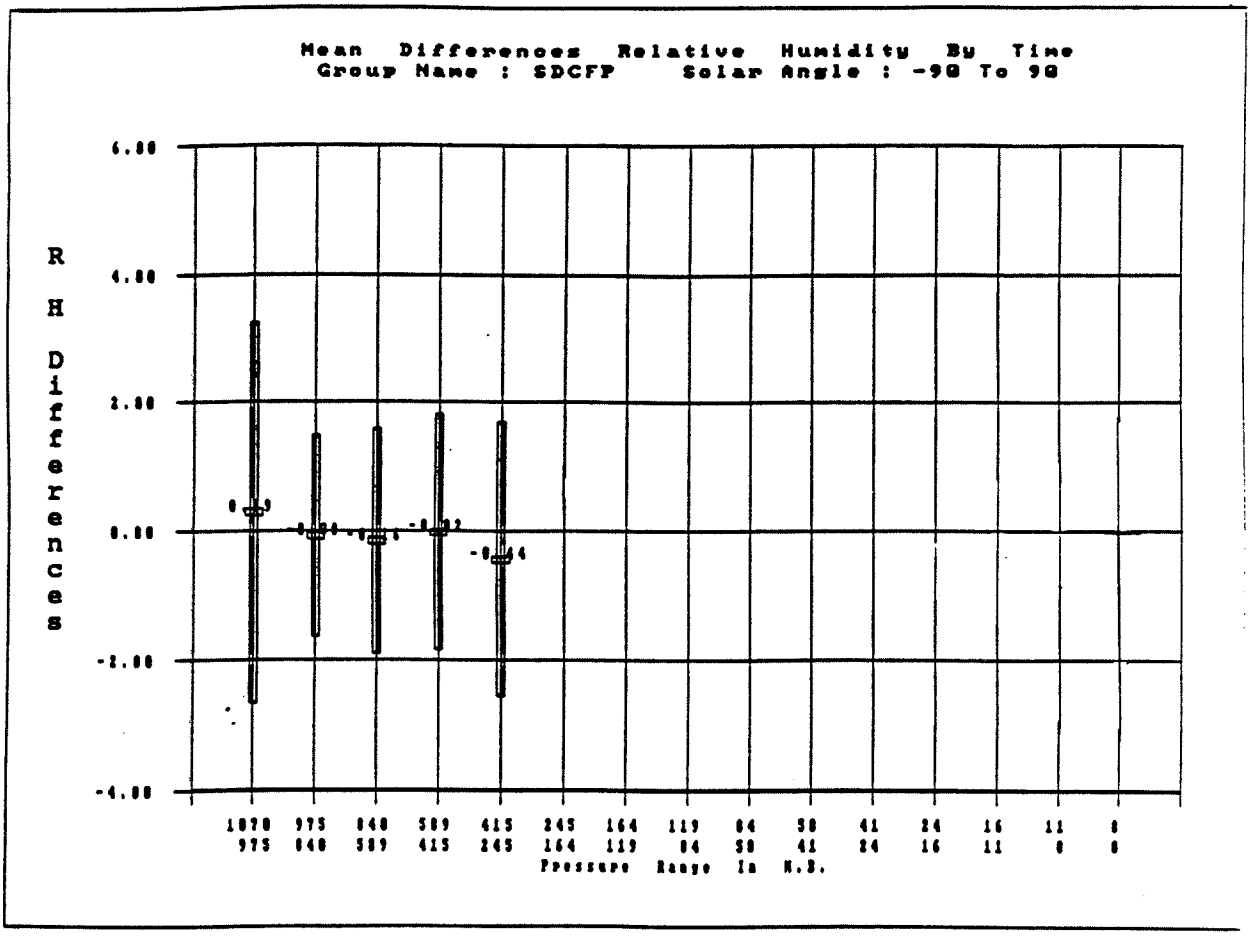

Figure 9. Mean/std. deviation of Relative Humidity Difference within selected pressure layers. Plotted values are mean differences (%R.H.). Bar gives +/- 1 std. deviation. Sampled at same time of flight.

FROM	MB.	TO	SAMPLE SIZE	# OF FLIGHTS	PRIMARY MEAN	SECONDARY MEAN	MEAN DIFF	RMS DIFF	STD DIFF
975.0	THRU	1069.9	55	35	67.90	67.62	.29	2.94	2.95
840.0	THRU	974.9	215	45	71.70	71.79	-.08	1.57	1.57
589.0	THRU	839.9	469	44	53.96	54.12	-.16	1.76	1.75
415.0	THRU	588.9	420	44	47.42	47.43	-.02	1.83	1.83
245.0	THRU	414.9	363	42	41.05	41.49	-.44	2.17	2.13

Table 9. Mean, rms (functional precision), and std. dev. of Relative Humidity Difference within selected pressure layers. Sampled at same time of flight.

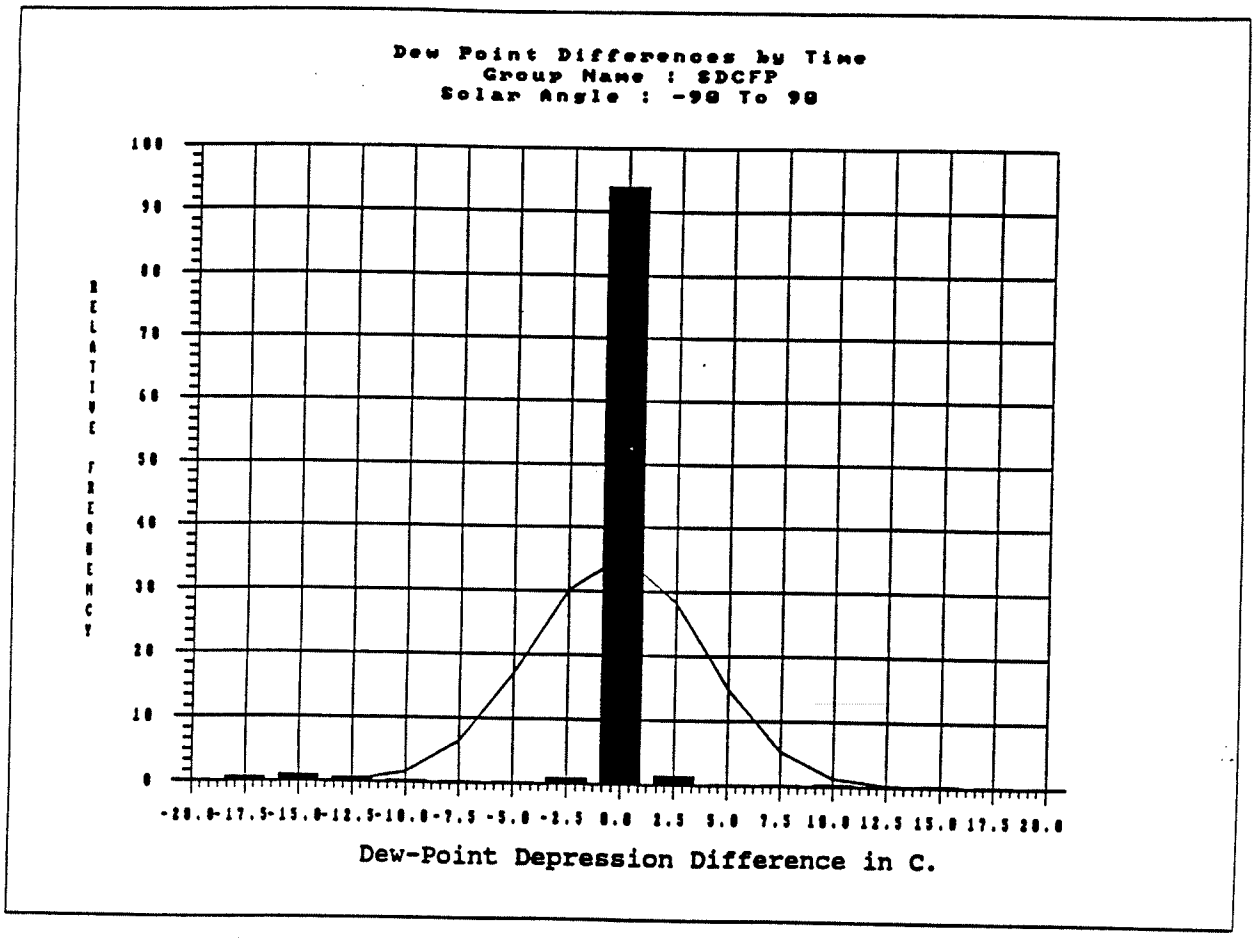

Figure 10. Histogram of Dew-Point Depression Difference sampled at same time of flight. Noraml curve computed from sample mean and std. dev.

SAMPLE SIZE	# OF FLIGHTS	MEAN DIFF	STD DEV DIFF	RMS DIFF	SKEW. DIFF	KURT. DIFF	CORR. P & S	PRIM MIN	PRIM MAX	SECOND MIN	SECOND MAX	DIFFER MIN	DIFFER MAX
1598.0	45	-.20	2.79	2.80	-2.64	29.71	.96	.20	30.00	.30	30.00	-24.30	16.90

Table 10. Dew-Point Depression sampled at same time of flight. Mean, std. dev., rms (functional precision), skewness, and kurtosis of differences. 'Primary sonde' and 'secondary sonde' correlation. Minimum and maximum Dew-Point Depression and Dew-Point Depression Difference in degrees C.

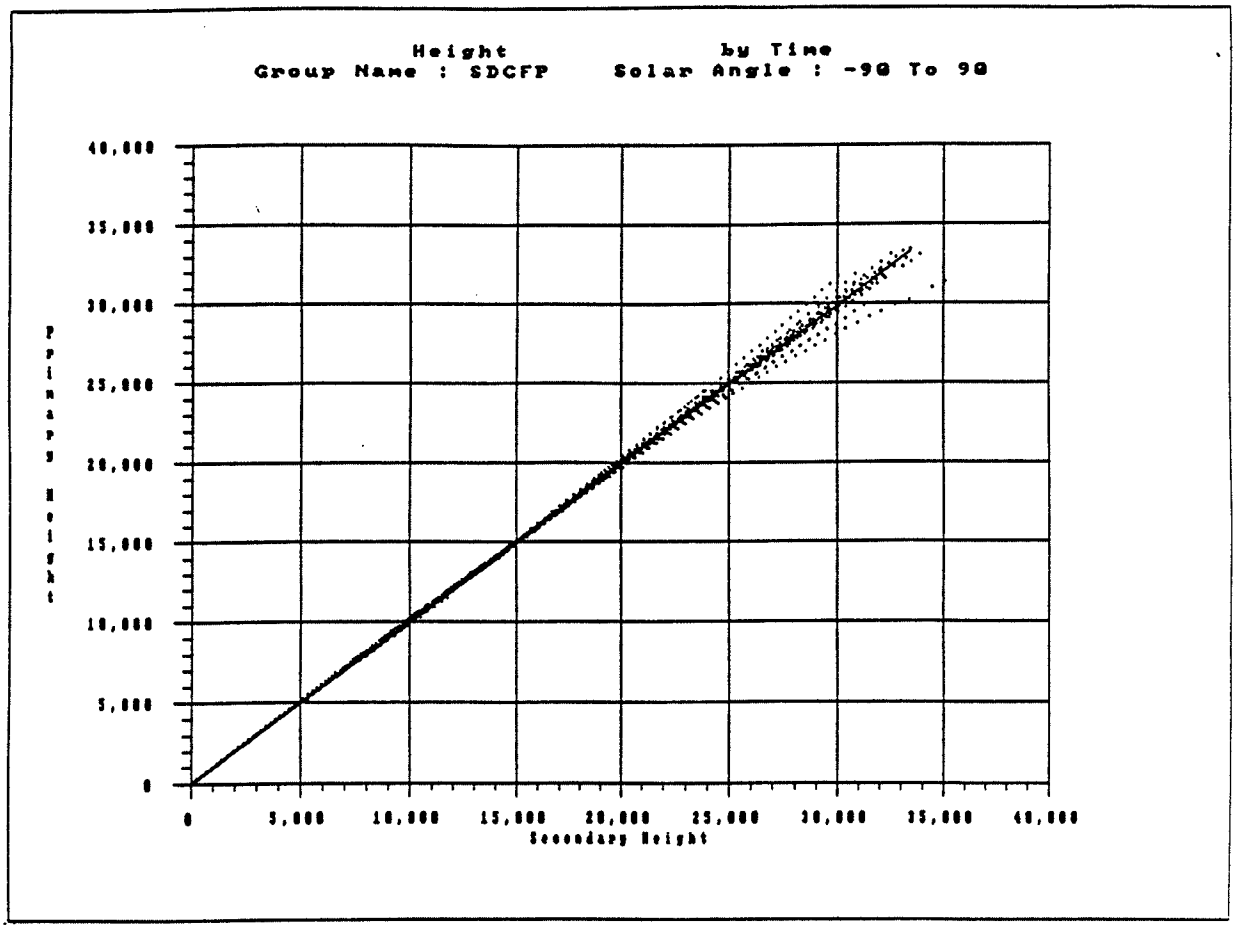

Figure 11. Scatter plot of 'primary sonde' Height versus 'secondary sonde' Height sampled at same time of flight. Regression line also plotted.

SAMPLE SIZE	# OF FLIGHTS	MEAN DIFF	STD DEV DIFF	RMS DIFF	SKEW. DIFF	KURT. DIFF	CORR. P & S	PRIM MIN	PRIM MAX	SECOND MIN	SECOND MAX	DIFFER MIN	DIFFER MAX
3571.0	45	-14.44	231.36	231.81	-4.93	72.25	1.00	103.80	33444.8	103.80	35111.3	-3738.4	1682.10

Table 11. Height sampled at same time of flight. Mean, std. dev., rms, skewness, and kurtosis of differences. 'Primary sonde' and 'secondary sonde' correlation. Minimum and maximum Height Difference in meters.

5. COMPARISON BY PRESSURE

Comparisons by pressure are more useful to the operational meteorologist since they represent the functional precision of radiosonde data at a specific pressure. The derived statistics can be directly applied to constant-pressure analysis and forecast model initialization. For dual flights, two radiosondes can report different pressures at the same time if their pressure sensors have different response characteristics. In this case, the comparisons of temperature, relative humidity, or dew point depression made at the same reported pressure will be taken at slightly different times and produce different statistics. For example, at the surface, a 1 mb pressure difference results in an approximate 2 second time difference. However, at 10 mb, this results in an approximate 1 minute time difference. This time difference contributes to the overall measurement differences and, consequently, tend toward worse precisions (i.e., larger σ-D's).

However, height precisions by pressure are significantly better than precisions by time. This is because height is not directly measured by the radiosonde but is derived using the hypsometric equation and, therefore, is a function of its measured pressure and mean virtual temperature. Comparing height calculations from measurements made by two sondes at the same time, the height discrepancies are caused by the differences in measured pressures and mean virtual temperatures. However, if height calculations using measurements made at the same measured pressure are compared, no difference in the measured pressures occur and only the difference in mean virtual temperatures remains. Since the mean virtual temperature calculation is insensitive to small time differences when the sonde measures a common pressure, the discrepancies in height are significantly less than those compared at the same time and, consequently, the functional precision is better (smaller σ-D).

5.1 TEMPERATURE

For the total population, 83.9% of the temperature differences by pressure were within ±0.5°C (Figure 12, Table 12). As was done for data at the same time, relative frequencies for the magnitude of temperature difference occurring within a difference interval are given for 7 temperature intervals (Table 12). Note that the sample sizes are much smaller than for the comparisons by pressure.

The scatter plot for temperature by pressure (Figure 13) shows a few more outliers than that by time (Figure 5). Most occur at temperatures below -40°C, as would be expected given the time effects on comparisons by pressure as discussed in section 5.

The overall functional precision (σ-D) for temperature by pressure is 0.68°C (Table 12). For the 7 temperature intervals, precisions ranged from 0.29°C between -20 and -5°C to a value of 0.84°C between -60 and -40°C. For the interval 20 to 35°C, the sample size is small and the precision should be used with caution. Precisions and other statistics for various pressure levels were computed (Table 18a). Sample sizes were small and the statistics should be used with caution.

5.2 HUMIDITY

Relative humidity is measured by the radiosonde hygristor in terms of electrical resistance. It is converted to dew-point depressions for message coding and transmission to other users. To determine a measure of humidity from the dew-point depression, the temperature must be known, so, if the temperatures reported by both sondes used in the comparisons are not the same, the dew-point depression differences do not give a pure measure of the humidity statistics but rather a combined measure of temperature and humidity statistics which are difficult to objectively analyze.

5.2.1 RELATIVE HUMIDITY

For the total population, 96.4% of the relative humidity differences by pressure were within ±5.0% RH (Figure 14, Table 14).

Except for fewer points, the scatter plot (Figure 15) does not look much different from that for relative humidity sampled by time (Figure 8). As stated earlier, accuracies of relative humidities below 20 percent calculated using current NWS equations is questionable so the precision at these values may not reflect optimal performance.

The overall functional precision (σ-D) for relative humidity differences by pressure is 2.2% (Table 14). Precision and other statistics for various pressure levels were computed (Table 18b). Sample sizes were small and the statistics should be used with caution.

5.2.2 DEW-POINT DEPRESSION

Overall functional precision (σ-D) for dew-point depression by pressure is 3.4°C (Table 16). Refer to section 4.4 for comments on the validity of these precision numbers.

5.3 HEIGHT

The scatter plot of heights compared by pressure (Figure 17) contains no outlier points, indicating good precision throughout the range. This precision is important to meteorological operations since numerical models are highly sensitive to inconsistencies and errors in pressure-level height calculations based on radiosonde observations. The scatter of heights by pressure can be compared with the scatter of heights by time (Figure 11), which show significantly more scatter.

The overall functional precision (σ-D) for the height by pressure is 16.3 meters (Table 17). Precision and other statistics for selected pressure levels are given (Table 18c). Theses statistics are based on small sample sizes and should be used with caution. Below 900 mb, the precision of the pressure heights is within 1 meter, above 900 mb the precision gradually increases reaching 10 meters near 300 mb, 20 meters near 60 mb, 24 meters near 40 mb, and 30 meters near 30 mb.

Comparing absolute height difference with height produced a strong correlation of 0.54 (i.e., more height scatter at increasing heights).

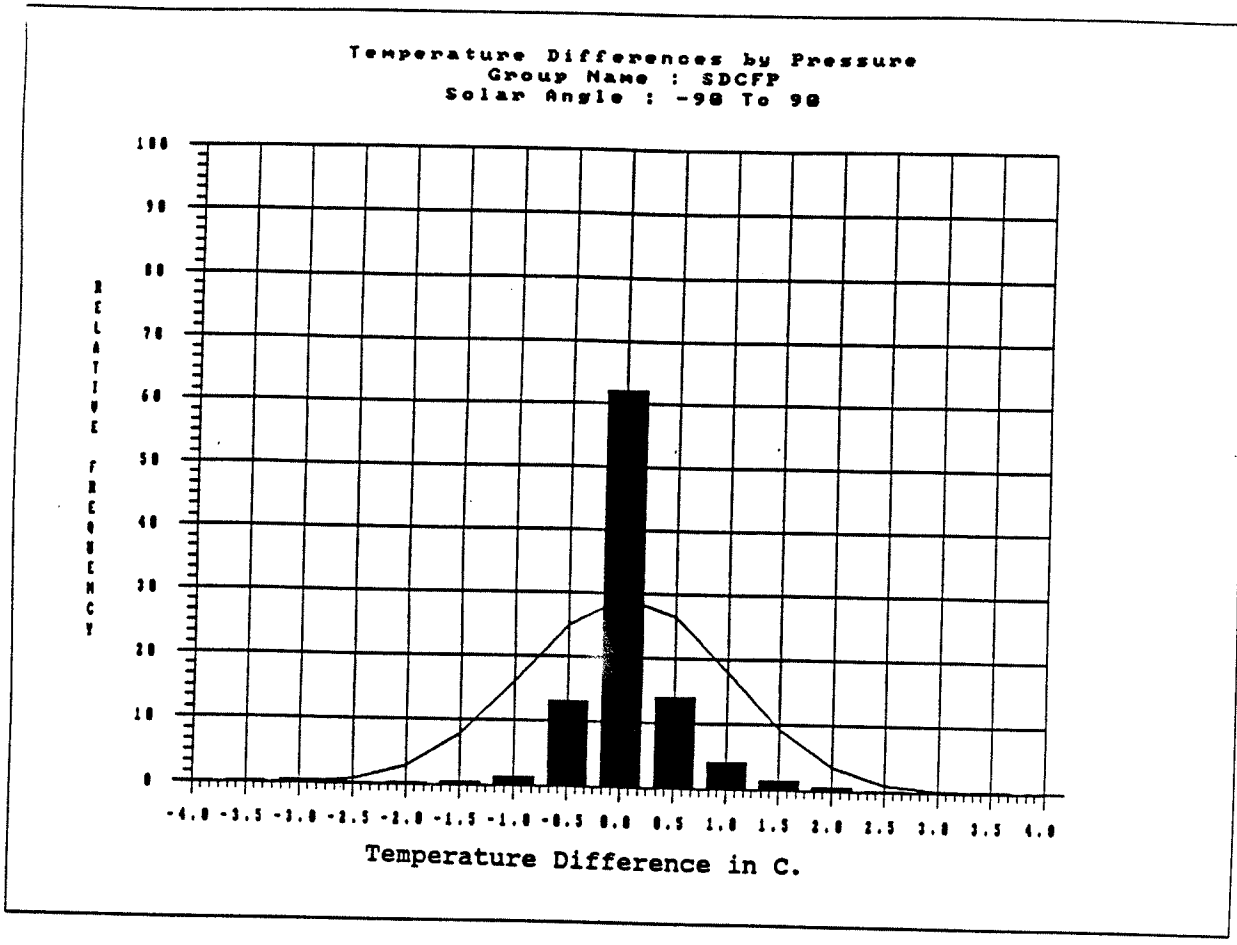

Figure 12. Histogram of Teperature Difference sampled at same pressure. Noral curve computed from sample mean and standard deviation.

FROM	DEG.	TO	SAMPLE SIZE	# OF FLIGHTS	Absolute Temperature Difference Interval 0.0-0.5	0.6-1.0	1.1-1.5	1.6-2.0	2.1-2.5	2.6-3.0	> = 3.1	MEAN DIFF.	RMS DIFF.	STD.DEV. DIFF.
					Relative Frequency in %									
20.0	THRU	34.9	21	13	76.2	19.0	0.0	0.0	0.0	0.0	4.8	.28	.98	.96
5.0	THRU	19.9	87	33	93.1	4.6	1.1	0.0	0.0	0.0	1.1	.11	.59	.58
-5.0	THRU	4.9	93	39	92.5	6.5	0.0	0.0	0.0	1.1	0.0	-.01	.39	.39
-20.0	THRU	-5.1	121	44	91.7	7.4	.8	0.0	0.0	0.0	0.0	.02	.28	.29
-40.0	THRU	-20.1	119	44	82.4	10.1	3.4	.8	.8	.8	1.7	.05	.78	.78
-60.0	THRU	-40.1	291	44	77.0	12.7	3.8	2.7	.7	.3	2.7	.06	.84	.84
-90.0	THRU	-60.1	101	34	82.2	11.9	3.0	2.0	0.0	0.0	1.0	.05	.57	.57
	ALL		833	45	83.9	10.1	2.4	1.3	.4	.4	1.6	.05	.68	.68

Table 12. Frequency of occurrence (%) of Absolute Temperature Difference within selected temperature intervals and for all data. Mean, rms (functional precision), and std. dev. of Temperature Difference for layers and all data. Sampled at same pressure.

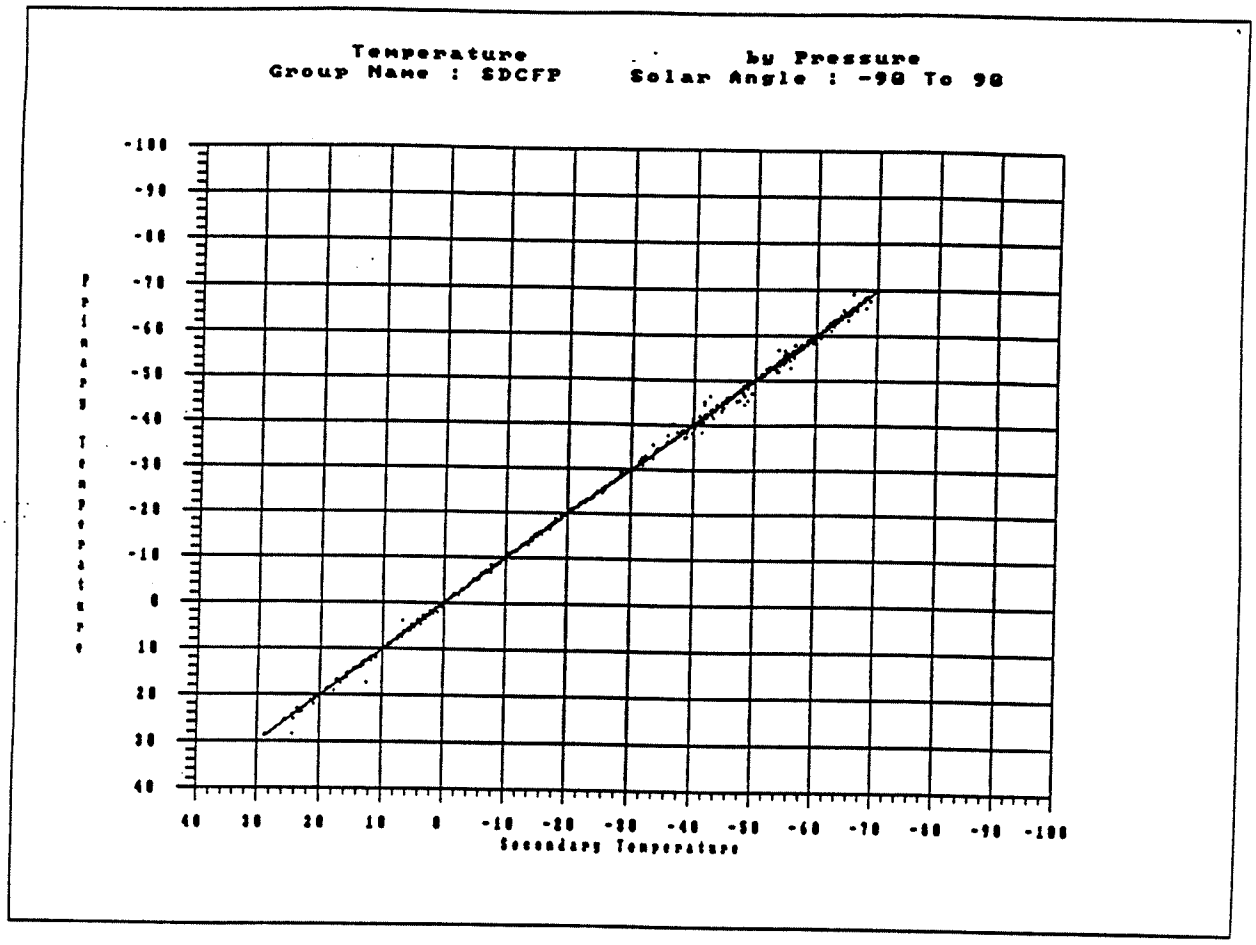

Figure 13. Scatter plot of 'primary sonde' Temperature versus 'secondary sonde' Temperature sampled at same pressure. Regression line also plotted.

SAMPLE SIZE	# OF FLIGHTS	MEAN DIFF	STD DEV DIFF	RMS DIFF	SKEW. DIFF	KURT. DIFF	CORR. P & S	PRIM MIN	PRIM MAX	SECOND MIN	SECOND MAX	DIFFER MIN	DIFFER MAX
833.00	45	.05	.68	.68	1.34	21.13	1.00	-70.20	28.60	-70.10	28.80	-3.80	5.20

Table 13. Temperature sampled at same pressure. Mean, std. dev., rms, skewness, and kurtosis of differences. 'Primary sonde' and 'secondary sonde' correlation. Minimum and maximum Temperature and Temperature Difference in degrees C.

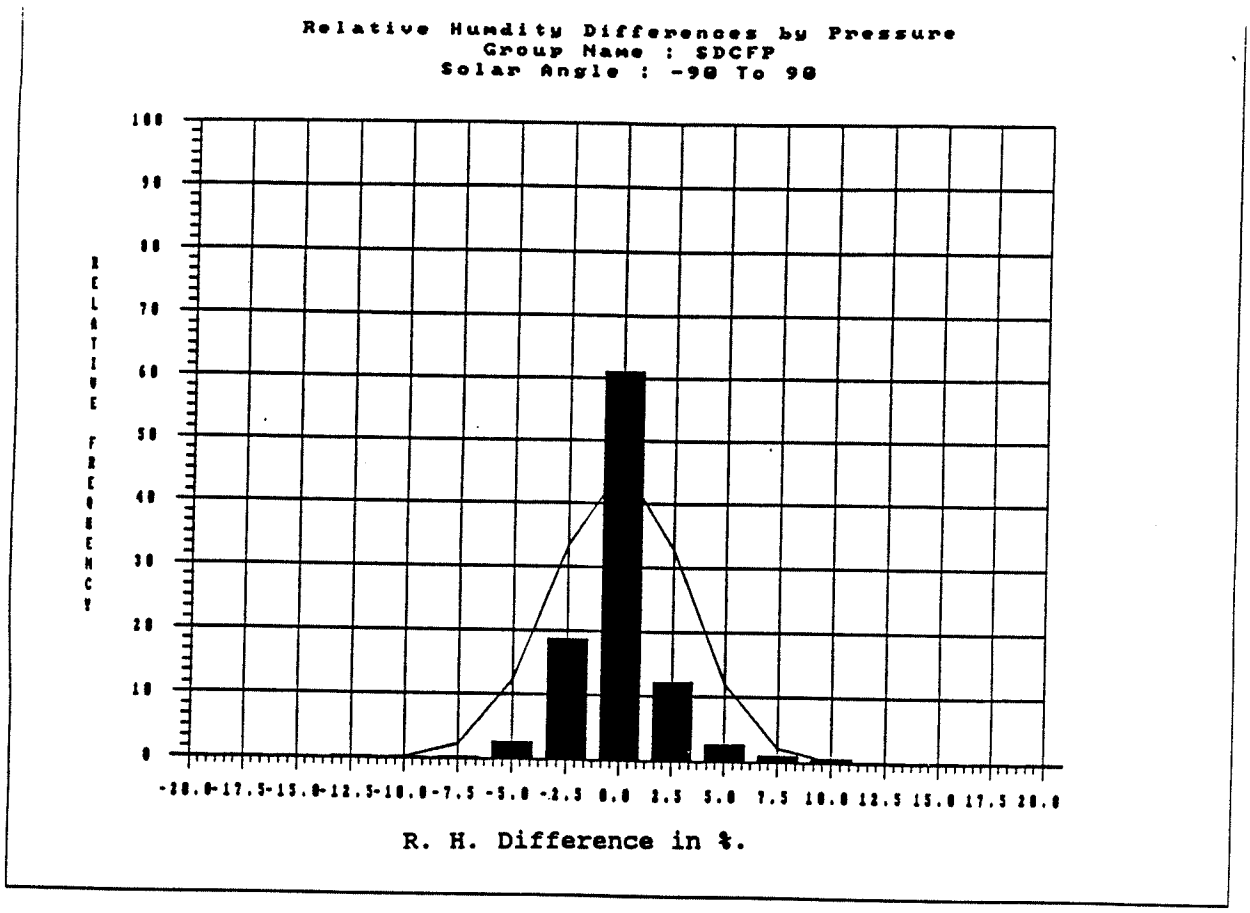

Figure 14. Histogram of Relative Humidity Difference sampled at same pressure. Normal curve computed from sample mean and std. dev.

FROM	PERC	TO	SAMPLE SIZE	# OF FLIGHTS	Absolute R. H. Difference Interval 0.0-2.5	2.6-5.0	5.1-7.5	7.6-10.0	10.1-12.5	12.6-15.0	> = 15.0	MEAN DIFF.	RMS DIFF.	STD.DEV. DIFF.
					Relative Frequency in %									
90.0	THRU	100.0	77	28	85.7	10.4	0.0	2.6	1.3	0.0	0.0	.65	2.44	2.37
80.0	THRU	89.9	38	27	84.2	10.5	2.6	2.6	0.0	0.0	0.0	.32	2.24	2.25
70.0	THRU	79.9	32	21	96.9	3.1	0.0	0.0	0.0	0.0	0.0	-.64	1.32	1.18
60.0	THRU	69.9	33	18	90.9	6.1	3.0	0.0	0.0	0.0	0.0	-.15	1.65	1.67
50.0	THRU	59.9	28	20	71.4	17.9	7.1	3.6	0.0	0.0	0.0	.41	2.89	2.92
40.0	THRU	49.9	44	22	75.0	20.5	4.5	0.0	0.0	0.0	0.0	-1.21	2.47	2.19
30.0	THRU	39.9	47	24	89.4	8.5	2.1	0.0	0.0	0.0	0.0	.10	1.69	1.70
20.0	THRU	29.9	66	24	81.8	13.6	3.0	1.5	0.0	0.0	0.0	.42	2.22	2.20
10.0	THRU	19.9	72	22	94.4	4.2	0.0	0.0	1.4	0.0	0.0	-.37	1.88	1.85
00.0	THRU	09.9	4	1	0.0	100.0	0.0	0.0	0.0	0.0	0.0			
	ALL		441	45	85.3	11.1	2.0	1.1	.5	0.0	0.0	-.03	2.16	2.17

Table 14. Frequency of occurrence (%) of Absolute Relative Humidity Difference within selected relative humidity intervals and for all data. Mean, rms (functional precision), and std. dev. of Relative Humidity Difference for layers and all data. Sampled at same pressure.

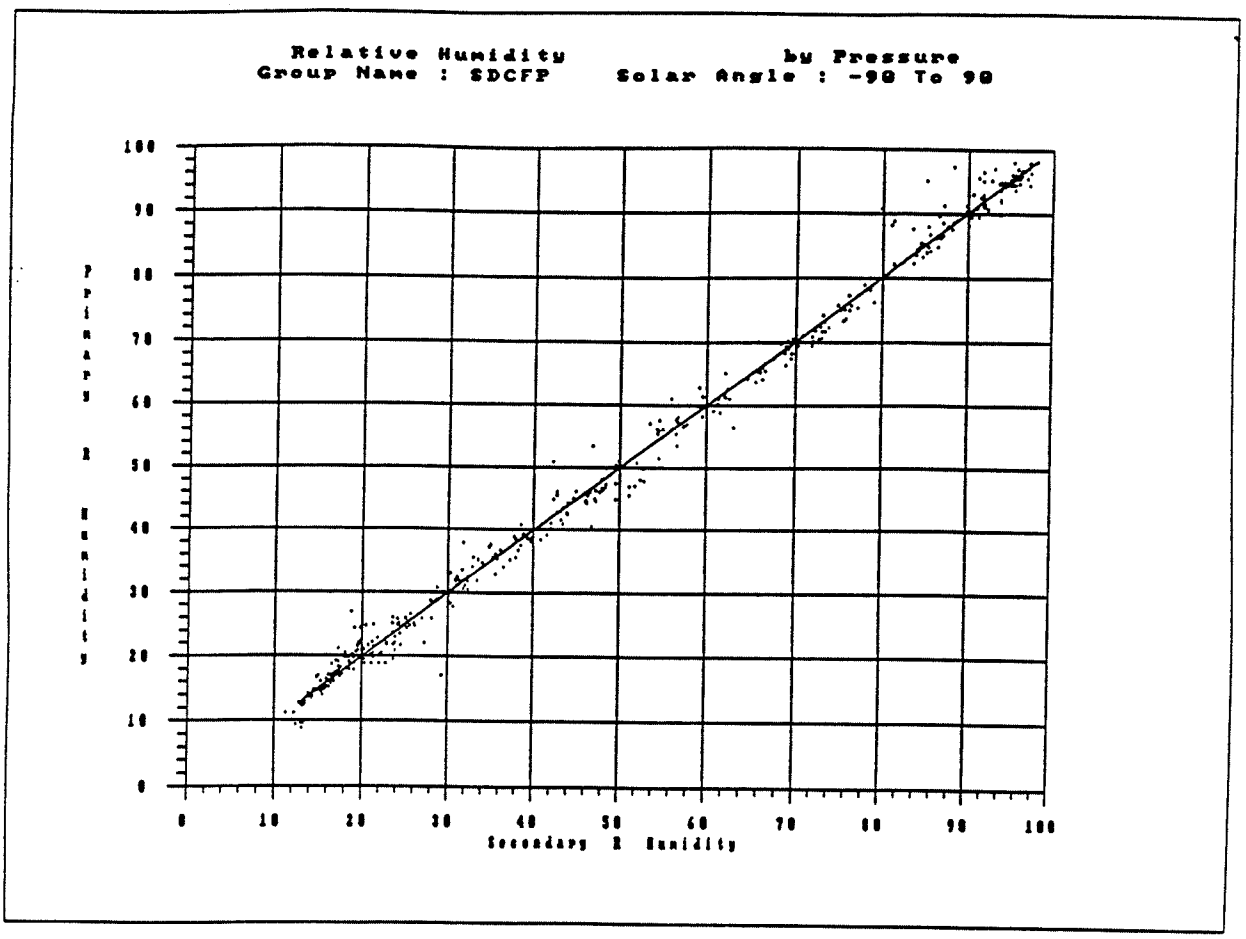

Figure 15. Scatter plot of 'primary sonde' Relative Humidity versus 'secondary sonde' Relative Humidity sampled at same pressure. Regression line also plotted.

SAMPLE SIZE	# OF FLIGHTS	MEAN DIFF	STD DEV DIFF	RMS DIFF	SKEW. DIFF	KURT. DIFF	CORR. P & S	PRIM MIN	PRIM MAX	SECOND MIN	SECOND MAX	DIFFER MIN	DIFFER MAX
441.00	45	-.03	2.16	2.16	.75	9.53	1.00	9.00	98.20	11.30	98.20	-12.30	11.10

Table 15. Relative Humidity sampled at same pressure. Mean, std. dev., rms, skewness, and kurtosis of differences. 'Primary sonde' and 'secondary sonde' correlation. Minimum and maximum Relative Humidity and Relative Humidity Difference in percent.

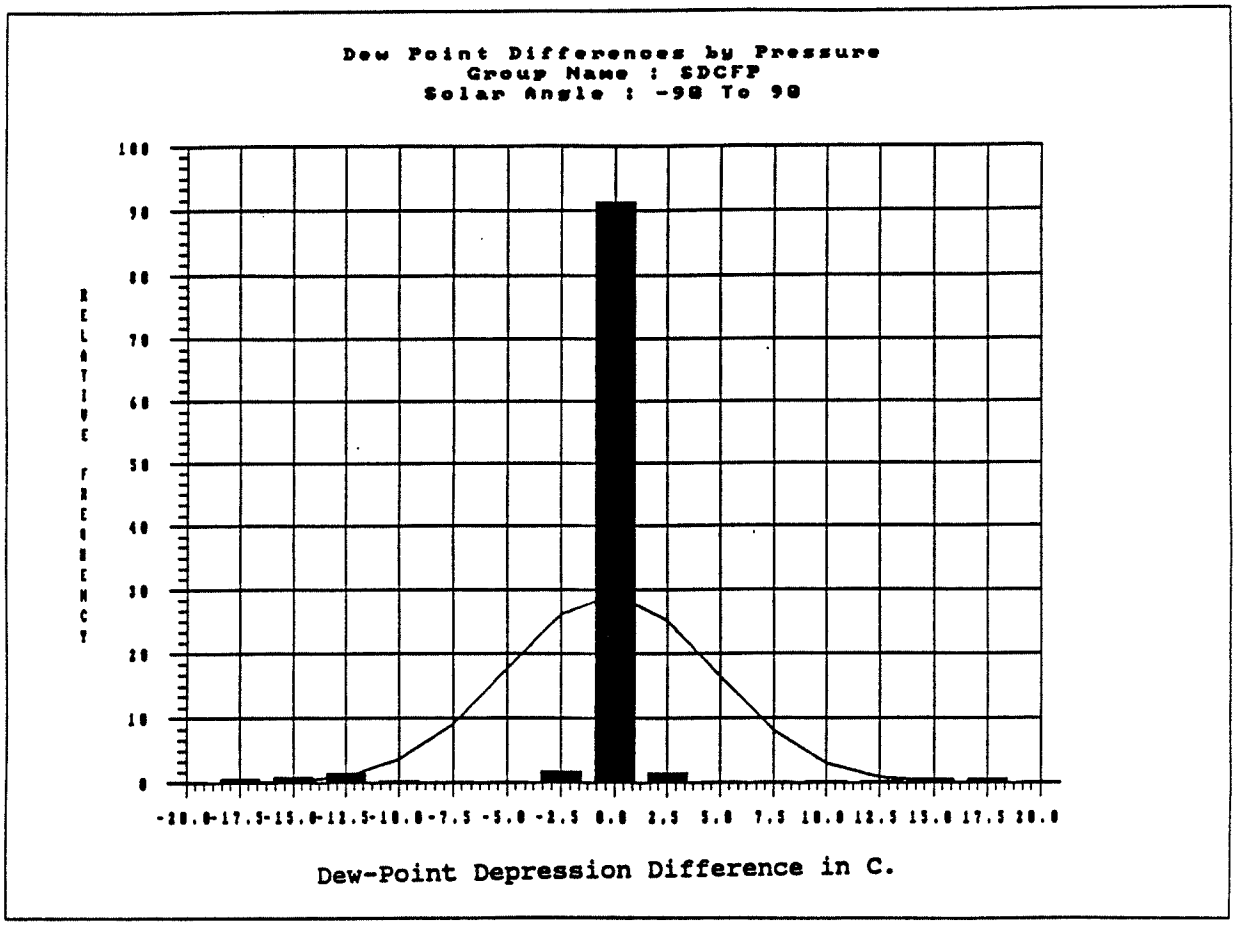

Figure 16. Histogram of Dew-Point Depression Difference sampled at same pressure. Normal curve computed from sample mean and std. dev.

SAMPLE SIZE	# OF FLIGHTS	MEAN DIFF	STD DEV DIFF	RMS DIFF	SKEW. DIFF	KURT. DIFF	CORR. P & S	PRIM MIN	PRIM MAX	SECOND MIN	SECOND MAX	DIFFER MIN	DIFFER MAX
441.00	45	-.18	3.40	3.40	-.74	20.01	.94	.30	30.00	.30	30.00	-17.30	17.30

Table 16. Dew-Point Depression sampled at same pressure. Mean, std. dev., rms, skewness, and kurtosis of differences. 'Primary sonde' and 'secondary sonde' correlation. Minimum and maximum Dew-Point Depression and Dew-Point Depression Difference in degrees C.

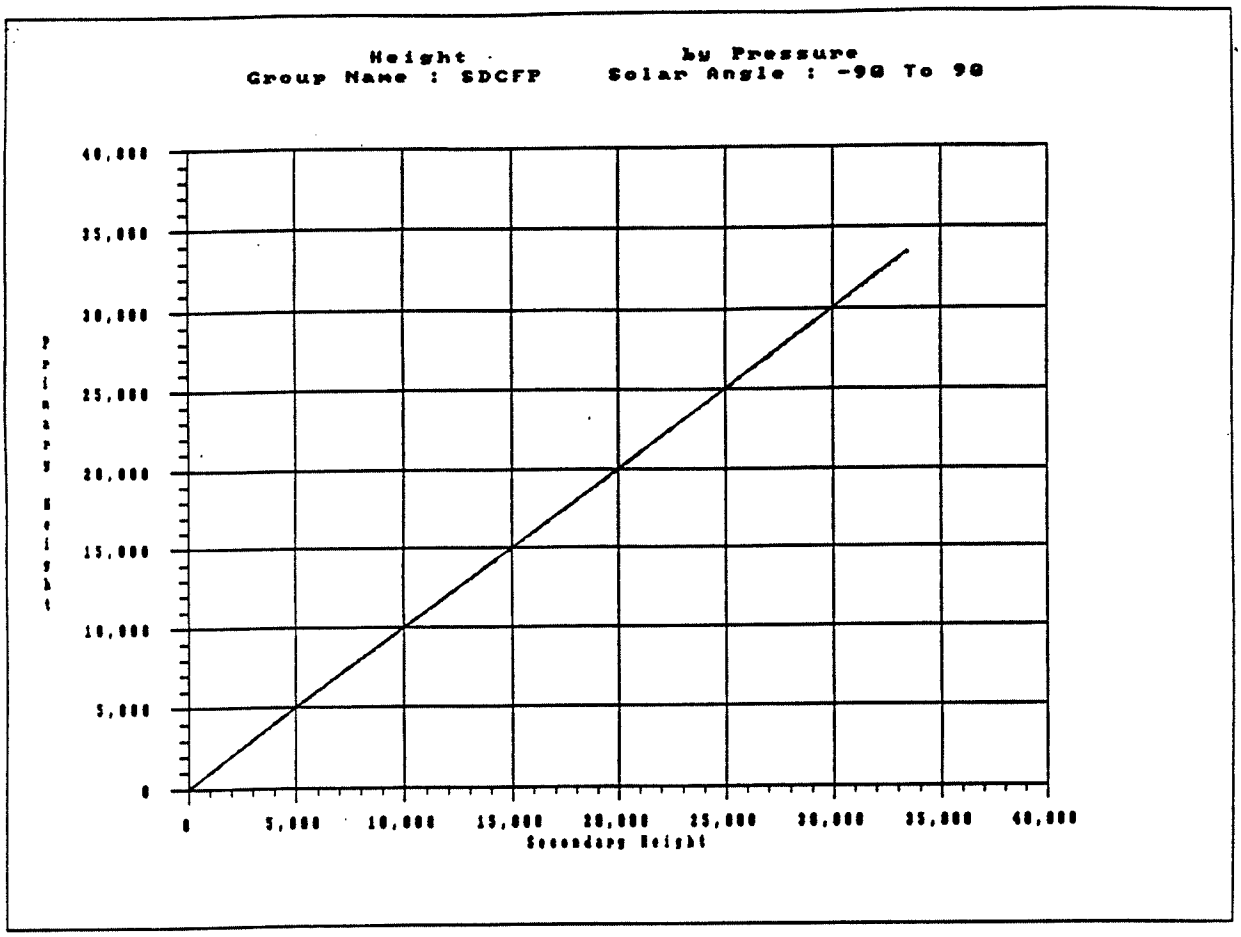

Figure 17. Scatter plot of 'primary sonde' Height versus 'secondary sonde' Height sampled at same pressure. Regression line also plotted.

SAMPLE SIZE	# OF FLIGHTS	MEAN DIFF	STD DEV DIFF	RMS DIFF	SKEW. DIFF	KURT. DIFF	CORR. P & S	PRIM MIN	PRIM MAX	SECOND MIN	SECOND MAX	DIFFER MIN	DIFFER MAX
833.00	45	1.90	16.16	16.27	1.76	12.42	1.00	90.50	33489.7	90.50	33508.0	-63.50	103.40

Table 17. Height sampled at same pressure. Mean, std. dev., rms, skewness, and kurtosis of differences. 'Primary sonde' and 'secondary sonde' correlation. Minimum and maximum Height and Height Difference in meters.

Table 18 a.

SDC Temperature Sensor Functional Precision Statistics
at Various Pressure Levels

Pressure (mb)	Sample Size	Temperature Difference: [Mean	σ-D	Kurt	Abs Max]	Temperature Range:
1000	37	.11	.97	16.34	4.7	27.9 to -8.5
900	45	.03	.29	11.86	1.4	21.5 to -15.2
850	44	.01	.25	3.30	.7	18.2 to -19.3
700	44	.04	.26	3.64	.7	8.2 to -21.0
600	44	.02	.22	6.96	.8	2.2 to -25.7
500	43	-.03	.34	8.30	1.3	-6.0 to -30.6
400	44	-.03	.32	4.39	1.0	-16.5 to -42.3
300	44	-.03	.36	6.71	1.3	-31.0 to -51.4
250	43	-.03	.63	14.36	3.1	-40.7 to -57.7
200	40	.01	.40	4.54	1.2	-45.2 to -63.5
150	36	.13	.44	7.86	1.9	-48.6 to -68.1
100	34	-.03	.48	3.49	1.3	-56.0 to -70.1
80	31	.08	.45	4.11	1.3	-56.3 to -68.5
60	29	.13	.79	6.62	2.9	-52.9 to -70.2
50	25	.20	.58	5.62	1.7	-50.0 to -66.5
40	24	.11	.73	5.79	2.1	-47.5 to -68.7
20	19	.57	1.09	3.97	3.5	-39.9 to -56.2
15	17	.61	1.99	4.02	5.2	-36.7 to -48.9
10	5	-.16	.71	1.99	1.2	-32.5 to -40.6
9	5	-.54	.73	2.05	1.8	-31.7 to -39.8
8	4	-.65	.91	2.27	2.2	-30.5 to -38.9

Table 18 b.

SDC Relative Humidity Sensor Functional Precision Statistics at Various Pressure Levels

Pressure (mb)	Sample Size	Humidity Difference: [Mean	σ-D	Kurt	Abs Max]	Humidity Range:
1000	37	.71	3.55	4.44	11.1	98.0 to 30.4
900	45	-.05	1.35	4.53	4.4	98.1 to 16.9
850	44	.02	1.32	6.62	4.7	98.2 to 15.3
700	44	-.04	1.84	10.11	8.1	97.2 to 13.8
600	44	.39	2.15	5.89	7.7	96.0 to 11.3
500	43	-.14	1.45	4.79	4.3	94.9 to 11.3
400	41	-.25	2.51	14.13	12.3	88.3 to 13.1
300	44	.25	1.76	6.08	6.0	74.8 to 14.0

Table 18 c.

SDC Height Calculation Functional Precision Statistics
at Various Pressure Levels

Pressure (mb)	Sample Size	Height Difference: [Mean	σ-D	Kurt	Abs Max]	Height Range:		
1000	37	.05	.37	23.44	1.7	278	to	91
900	45	.43	1.44	18.36	8.1	1144	to	928
850	44	.48	1.69	11.12	8.1	1637	to	1374
700	44	.62	2.78	5.97	10.2	3267	to	2861
600	44	.64	3.74	5.95	14.1	4525	to	4019
500	43	.57	5.15	5.95	18.9	5971	to	5345
400	44	.44	7.23	6.56	24.4	7683	to	6895
300	44	.35	10.43	8.18	41.4	9767	to	8819
250	43	.30	11.90	7.66	45.4	11018	to	10007
200	40	.73	14.49	7.40	54.7	12476	to	11441
150	36	2.10	16.72	6.81	60.0	14259	to	13286
100	34	1.22	16.47	5.95	57.2	16729	to	15830
80	31	.56	18.27	5.71	61.4	18111	to	17197
60	29	3.60	19.48	5.14	65.1	19947	to	18933
50	25	5.86	20.86	4.75	66.8	21117	to	20032
40	24	5.69	24.01	3.78	69.4	22578	to	21384
20	19	9.76	33.37	2.65	76.3	27233	to	25672
15	17	14.64	41.22	2.75	103.4	29199	to	27612
10	5	-10.04	16.78	1.87	37.7	31923	to	31403
9	5	.10	14.09	1.32	17.7	32658	to	32104
8	4	-7.38	39.96	1.98	63.5	33507	to	32950

6. SUMMARY/CONCLUSIONS

The following summary and conclusions were drawn from this set of functional precision tests:

The functional precision of Space Data Corporation Model 909-10-01 (SDC) radiosonde was determined using the National Weather Service functional analysis test package. The comparisons were made from 45 flights of paired radiosondes suspended from the same balloon. The two sondes were vertically separated by about 10 meters and, for this report, functional precision is given by the standard deviation of the differences (σ-D) between measurements made by 2 sensors of the same type exposed to the same environment. Results are summarized for simultaneous measurements at one minute intervals as well as measurements at a predefined set of pressure levels. These tests were conducted for the acceptance of contract production samples and results are reported here for use by the meteorological community in specifying the characteristics of this radiosonde which began operational use in February of 1989.

For comparisons made at one minute intervals, the overall functional precision for temperature was 0.3°C and ranged from 0.2 to 0.4°C. For altitudes below the 100 mb level, the precision for pressure ranged from 1.3 to 3.0 mb and 1.3 to 1.6 mb above, with an overall value of 2.1 mb. Relative humidity precision was 2%.

For comparisons made at predefined pressure levels, the functional precision for height ranged from 2 meters at 850 mb to 16 meters at 100 mb and 33 meters at 20 mb. For altitudes below 100 mb, the temperature precision ranged from 0.2 to 1.0°C and from 0.5 to 2.0°C above. Relative humidity precisions ranged from 1 to 4%.

Compared to the VIZA (Model 1492-510) time commutated sonde, precisions for data sampled at the same time for dew-point depression improved, for temperature and humidity were about the same and worsened for pressure. Both tests used the same automated data recording and reduction methods. Differences in performance are mainly attributed to the radiosonde design and sensor differences.

For these tests, the impact of the 30 foot vertical separation on the reported functional precisions is probably insignificant, except in the case of temperature precision near the surface when large lapse rates occur, the case of temperature precision for the -71 to -60°C interval where balloon effects might have been a factor, and the case of relative humidity precision for the 40 to 50% RH interval where some flights experienced large differences as sondes exited clouds.

Vertical separation of the radiosondes complicates the analyses of data from dual flights and should be avoided in the future unless absolutely necessary.

Using the standard deviation minimizes biases due to the vertical separation, but non-systematic effects cannot be eliminated.

The utility of a new micro-computer based integrated system for graphical and statistical analyses of dual radiosonde data was demonstrated.

7. REFERENCES

Ahnert, P.R., 1991: Precision and Comparability of National Weather Service Upper-Air Measurements. Proceedings Seventh AMS Symposium on Meteorological Observations and Instrumentation. January 14-18, 1991 New Orleans, LA. pp.221-226. American Meteorological Society, Boston, MA.

Hoehne, W.E., 1971: Standardized Functional Tests. NOAA Technical Memorandum NWS T&EL-12, Systems Development Office, Test and Evaluation Laboratory, Sterling, VA.

Hoehne, W.E., 1980: Precision of National Weather Service Upper-Air Measurements. NOAA Technical Memorandum NWS T&ED-16, Office of Systems Development, Test and Evaluation Division, Sterling, VA.

NWS, 1981: Federal Meteorological Handbook No. 3 - Radiosonde Observations. Second Edition, National Weather Service, Washington, D.C.

NWS, 1991a: Functional Precision of National Weather Service Upper-Air Measurements using VIZ Manufacturing Co. "A" Radiosonde (Model 1492-510). NOAA Technical Report NWS 44, Office of Systems Operations, Engineering Division, Test and Evaluation Branch, Sterling, VA.

NWS, 1991b: Functional Precision of National Weather Service Upper-Air Measurements using VIZ Manufacturing Co. "B" Radiosonde (Model 1492-520). NOAA Technical Report NWS 45, Office of Systems Operations, Engineering Division, Test and Evaluation Branch, Sterling, VA.

Ney, E.P., R.W. Maas, and W.F. Huch, 1961: The Measurement of Atmospheric Temperature. J. Met. Vol 18, February 1961. pp. 60-80

Schmidlin, F.J., J.K. Luers and P.D. Huffman, 1986: Preliminary Estimates of Radiosonde Thermistor Errors. NASA Technical Paper 2637, 15 p.

Tiefenau, H.K.E, and A. Gebbeken, 1989: Influence of Meteorological Balloons on Temperature Measurements with Radiosondes: Nighttime Cooling and Daylight Heating. J. Atmos. and Ocean. Tech., Vol 6, February, 1989, pp. 36-42

APPENDIX

Figure A1. Illustration of the Space Data Radiosonde (Model 909-10-01).

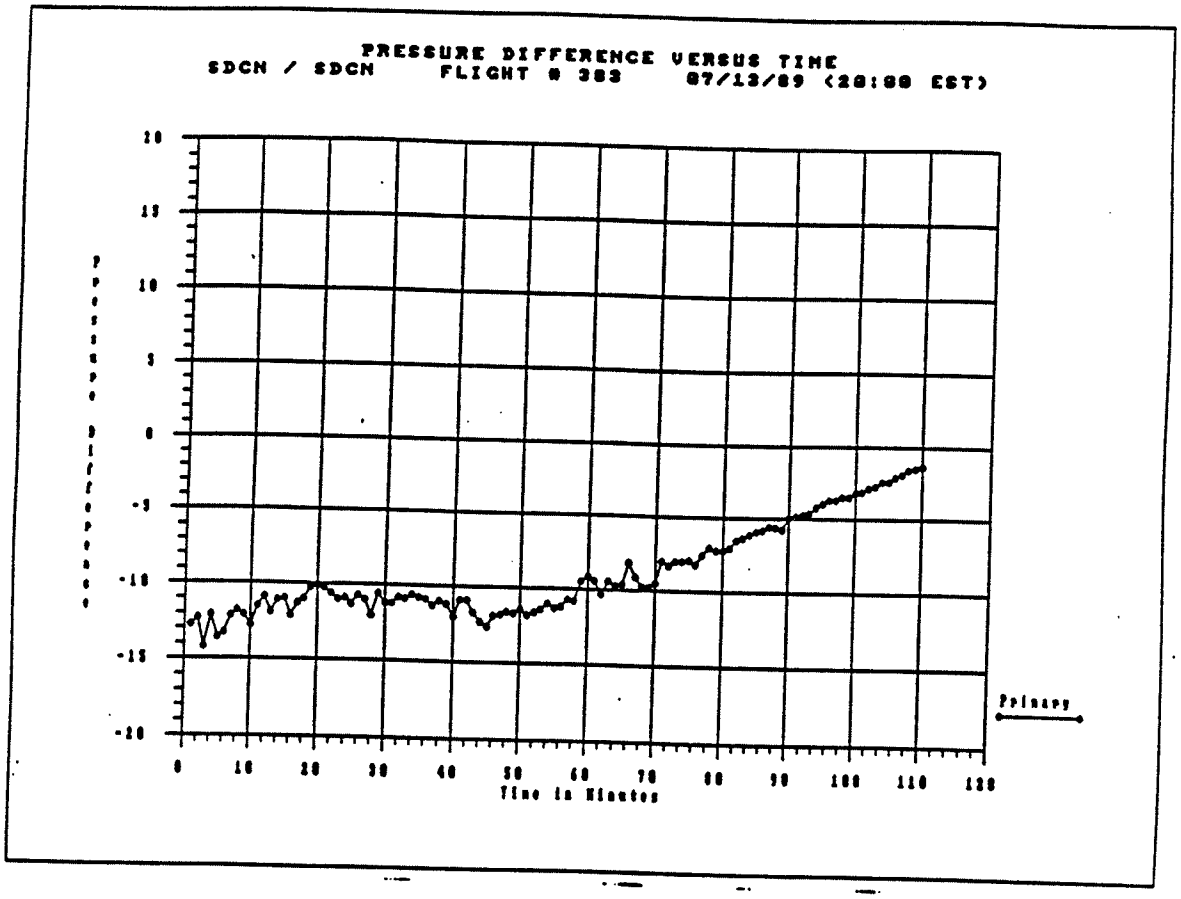
PRESSURE DIFFERENCE VERSUS TIME
SDCN / SDCN FLIGHT # 383 07/13/89 (20:00 EST)
Time In Minutes
Primary

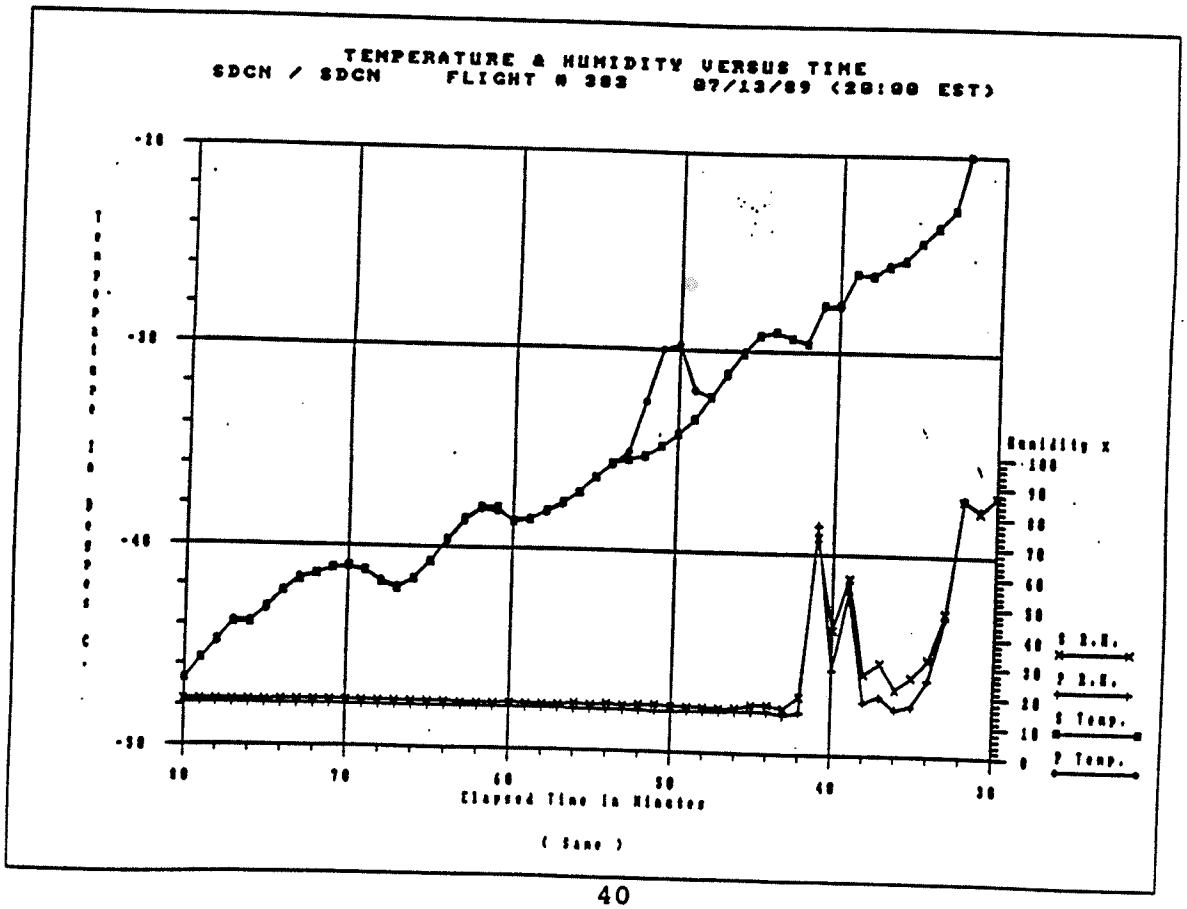
TEMPERATURE & HUMIDITY VERSUS TIME
SDCN / SDCN FLIGHT # 383 07/13/89 (20:00 EST)
Elapsed Time In Minutes
(Sane)

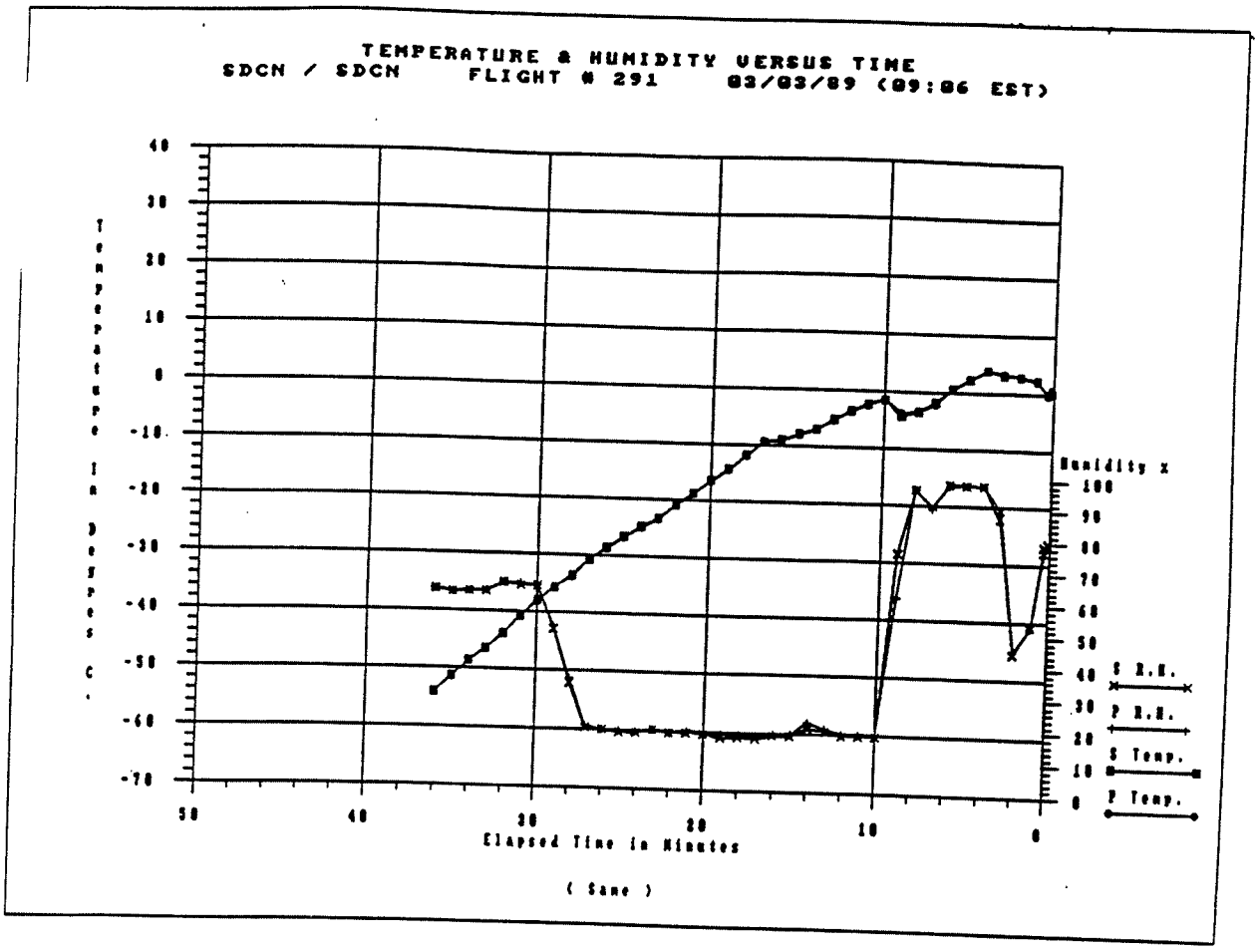
TEMPERATURE & HUMIDITY VERSUS TIME
SDCN / SDCN FLIGHT # 291 03/03/89 (09:06 EST)
Temperature in Degrees C.
40
30
20
10
0
-10
-20
-30
-40
-50
-60
-70
Humidity %
100
90
80
70
60
50
40
30
20
10
0
S R.H.
P R.H.
S Temp.
P Temp.
50
40
30
20
10
0
Elapsed Time in Minutes
(Sane)

(Continued from inside front cover)

NWS 18 Joint Probability Method of Tide Frequency Analysis Applied to Apalachicola Bay and St. George Sound, Florida. Francis P. Ho and Vance A. Myers, November 1975, 43 p. (PB-251123)

NWS 19 A Point Energy and Mass Balance Model of a Snow Cover. Eric Anderson, February 1976, 150 p. (PB-254651

NWS 20 Precipitable Water Over the United States, Volume I: Monthly Means. George A. Lott, November 1976, 173 p. (PB-264219)

NWS 20 Precipitable Water Over the United States, Volume II: Semimonthly Maxima. Francis P. Ho and John T. Riedel, July 1979, 359 p. (PB-300870)

NWS 21 Interduration Precipitation Relations for Storms - Southeast States. Ralph H. Frederick, March 1979, 66 p. (PB-297192)

NWS 22 The Nested Grid Model. Norman A. Phillips, April 1979, 89 p. (PB-299046)

NWS 23 Meteorological Criteria for Standard Project Hurricane and Probable Maximum Hurricane and Probable Maximum Hurricane Windfields, Gulf and East Coasts of the United States. Richard W. Schwerdt, Francis P. Ho, and Roger R. Watkins, September 1979, 348 p. (PB-80 117997)

NWS 24 A Methodology for Point-to-Area Rainfall Frequency Ratios. Vance A. Myers and Raymond M. Zehr, February 1980, 180 p. (PB80 180102)

NWS 25 Comparison of Generalized Estimates of Probable Maximum Precipitation With Greatest Observed Rainfalls. John T. Riedel and Louis C. Schreiner, March 1980, 75 p. (PB80 191463)

NWS 26 Frequency and Motion of Atlantic Tropical Cyclones. Charles J. Neumann and Michael J. Pryslak, March 1981, 64 p. (PB81 247256)

NWS 27 Interduration Precipitation Relations for Storms-- Western United States. Ralph H. Frederick, John F. Miller, Francis P. Richards, and Richard W. Schwerdt, September 1981, 158 p. (PB82 230517)

NWS 28 GEM: A Statistical Weather Forecasting Procedure. Robert G. Miller, November 1981, 103 p.

NWS 29 Analysis of Elements of the Marine Environment for the Atlantic Remote Sensing Land Ocean Experiment (ARSLOE) -- An Atlas for October 22 through October 27, 1980. Lawrence D. Burroughs, May 1982, 116 p. (PB82 251281)

NWS 30 The NMC Spectral Model. Joseph G. Sela, May 1982, 38 p. (PB83 115 113)

NWS 31 A Monthly Averaged Climatology of Sea Surface Temperature. Richard W. Reynolds, June 1982, 37 p. (PB83 115469)

NWS 32 Pertinent Meteorological and Hurricane Tide Data for Hurricane Carla. Francis P. Ho and John F. Miller, August 1982, 111 p. (PB83 118240)

NWS 33 Evaporation Atlas for the Contiguous 48 United States. Richard K. Farnsworth, Edwin S. Thompson, and Eugene L. Peck, June 1982, 26 p.

NWS 34 Mean Monthly, Seasonal, and Annual Pan Evaporation for the United States. Richard K. Farnsworth and Edwin S. Thompson, December 1982, 85 p. (PB83 161729)

NWS 35 Pertinent Meteorological Data for Hurricane Allen of 1980. Francis P. Ho and John F. Miller, September 1983, 73 p. (PB 272 112)

NWS 36 Water Available for Runoff for 1 to 15 Days Duration and Return Periods of 2 to 100 Years for Selected Agricultural Regions in the Northwest United States. Frank P. Richards, John F. Miller, Edward A. Zurndorfer, and Norma S. Foat, April 1983, 59 p. (PB84 120591)

NWS 37 The National Weather Service Hurricane Probability Program. Robert C. Sheets, April 1984, 70 p. (PB84 182757)

NWS 38 Hurricane Climatology for the Atlantic and Gulf Coasts of the United States. Francis P. Ho, James C. Su, Karen L. Hanevich, Rebecca J. Smith, and Frank P. Richards, April 1987, 195 p.

NWS 39 Monthly Relative Frequencies of Precipitation for the United States for 6-, 12-, and 24-H Periods. John S. Jensenius, Jr., and Mary C. Erickson, September 1987, 262 p.

NWS 40 An Eight-Year Climatology of Meteorological and SBUV Ozone Data. Ronald M Nagatani, Alvin J. Miller, Keith W. Johnson, and Melvyn E. Gelman. March 1988, 123 pp.

(Continued on reverse page)

NTIS does not permit return of items for credit or refund. A replacement will be provided if an error is made in filling your order, if the item was received in damaged condition, or if the item is defective.

Reproduced by NTIS
National Technical Information Service
U.S. Department of Commerce
Springfield, VA 22161

This report was printed specifically for your order from our collection of more than 2 million technical reports.

For economy and efficiency, NTIS does not maintain stock of its vast collection of technical reports. Rather, most documents are printed for each order. Your copy is the best possible reproduction available from our master archive. If you have any questions concerning this document or any order you placed with NTIS, please call our Customer Services Department at (703)487-4660.

Always think of NTIS when you want:
• Access to the technical, scientific, and engineering results generated by the ongoing multibillion dollar R&D program of the U.S. Government.
• R&D results from Japan, West Germany, Great Britain, and some 20 other countries, most of it reported in English.

NTIS also operates two centers that can provide you with valuable information:
• The Federal Computer Products Center - offers software and datafiles produced by Federal agencies.
• The Center for the Utilization of Federal Technology - gives you access to the best of Federal technologies and laboratory resources.

For more information about NTIS, send for our FREE *NTIS Products and Services Catalog* which describes how you can access this U.S. and foreign Government technology. Call (703)487-4650 or send this sheet to NTIS, U.S. Department of Commerce, Springfield, VA 22161. Ask for catalog, PR-827.

Name _____
Address _____
_____
_____
Telephone _____

- Your Source to U.S. and Foreign Government Research and Technology.